TOXICOLOGICAL SCIENCES **66,** 34–53 (2002)

A Physiologically Based Pharmacokinetic and Pharmacodynamic (PBPK/PD) Model for the Organophosphate Insecticide Chlorpyrifos in Rats and Humans

C. Timchalk,*[,1] R. J. Nolan,† A. L. Mendrala,‡ D. A. Dittenber,‡ K. A. Brzak,‡ and J. L. Mattsson†

**Battelle Pacific Northwest Division, Chemical Dosimetry, PO Box 999, Richland, Washington 99352; †Dow AgroSciences, 9330 Zionsville, Indianapolis, Indiana 46268; and ‡The Dow Chemical Co., Midland, Michigan 48674*

Received August 16, 2001; accepted November 28, 2001

A PBPK/PD model was developed for the organophosphate insecticide chlorpyrifos (CPF) (*O,O*-diethyl-*O*-[3,5,6-trichloro-2-pyridyl]-phosphorothioate), and the major metabolites CPF-oxon and 3,5,6-trichloro-2-pyridinol (TCP) in rats and humans. This model integrates target tissue dosimetry and dynamic response (i.e., esterase inhibition) describing uptake, metabolism, and disposition of CPF, CPF-oxon, and TCP and the associated cholinesterase (ChE) inhibition kinetics in blood and tissues following acute and chronic oral and dermal exposure. To facilitate model development, single oral-dose pharmacokinetic studies were conducted in rats (0.5–100 mg/kg) and humans (0.5–2 mg/kg), and the kinetics of CPF, CPF-oxon, and TCP were determined, as well as the extent of blood (plasma/RBC) and brain (rats only) ChE inhibition. In blood, the concentration of analytes followed the order TCP >> CPF >> CPF-oxon; in humans CPF-oxon was not quantifiable. Simulations were compared against experimental data and previously published studies in rats and humans. The model was utilized to quantitatively compare dosimetry and dynamic response between rats and humans over a range of CPF doses. The time course of CPF and TCP in both species was linear over the dose range evaluated, and the model reasonably simulated the dose-dependent inhibition of plasma ChE, RBC acetylcholinesterase (AChE), and brain (rat only) AChE. Model simulations suggest that rats exhibit greater metabolism of CPF to CPF-oxon than humans do, and that the depletion of nontarget B-esterase is associated with a nonlinear, dose-dependent increase in CPF-oxon blood and brain concentration. This CPF PBPK/PD model quantitatively estimates target tissue dosimetry and AChE inhibition and is a strong framework for further organophosphate (OP) model development and for refining a biologically based risk assessment for exposure to CPF under a variety of scenarios.

Key Words: **physiologically based pharmacokinetics; organophosphate insecticide; chlorpyrifos; esterase inhibition.**

Chlorpyrifos (*O,O*-diethyl-*O*-[3,5,6-trichloro-2-pyridyl] phosphorothioate, CAS Registry No. 2921–88–2) is the active ingredient in DURSBAN® and LORSBAN® insecticides. Thionophosphorus organophosphates (OP) are a major subgroup of broad spectrum OP insecticides that see widespread commercial application, and their primary toxicological effect is associated with the inhibition of acetylcholinesterase (AChE, EC 3.1.1.7) in both central and peripheral nerve tissues (Murphy, 1986; Sultatos, 1994). Phosphorothionates like chlorpyrifos (CPF) do not directly inhibit AChE, but must first be metabolized to the corresponding oxygen analog (CPF-oxon). The activation of CPF to CPF-oxon is mediated by cytochrome P450 mixed-function oxidases (CYP450), primarily within the liver. However, extrahepatic metabolism has been reported in other tissues, including brain (Chambers and Chambers, 1989; Guengerich, 1977). In addition, oxidative dearylation of CPF to 3,5,6-trichloro-2-pyridinol (TCP) and diethylthiophosphate represents a competing detoxification pathway that is likewise mediated by hepatic CYP450 (Ma and Chambers, 1994). Intestinal CYP450 metabolism of drugs can be substantial (Hall *et al.*, 1999; Obach *et al.*, 2001; Paine *et al.*, 1999; Schmiedlin-Ren, *et al.*, 1993; Watkins, 1992; Zhang *et al.*, 1999), and also are likely to be important contributors to CPF metabolism. Intestinal cells also contain multidrug resistance proteins (p-glycoproteins) that react to CPF-oxon, and would likely be an additional barrier to oxon absorption (Lanning *et al.*, 1996).

Detoxification reactions are believed to share a common phosphooxythiran intermediate and represent critical biotransformation steps required for toxicity (Neal, 1980). Differences in the ratio of activation to detoxification are believed to be associated with sensitivity to OPs (Ma and Chambers, 1994). Hepatic and extrahepatic A-esterase (A-EST, EC 3.1.1.1.2) can effectively metabolize CPF-oxon to TCP (nontoxic metabolite) and diethylphosphate without inactivating the enzyme (Sultatos and Murphy, 1983). B-Esterases (B-EST) such as carboxylesterase (CaE, EC 3.1.1.1), and butyrylcholinesterase (BuChE, EC 3.1.1.8) can likewise detoxify CPF-oxon; however, these B-ESTs become irreversibly bound (1:1 ratio) to the CPF-oxon and thereby become inactivated (Chanda *et al*., 1977; Clement, 1984). Studies in both humans and rodents indicate that TCP represents the primary metabolite of CPF, although glucuro-

Presented in part at the 37th annual meeting of the Society of Toxicology, March, 1998, Seattle, Washington.

[1] To whom correspondence should be addressed. Fax: (509) 376-9064. E-mail: charles.timchalk@pnl.gov.

nide and sulfate conjugates of TCP have likewise been observed (Bakke *et al*., 1976; Nolan *et al*., 1984).

Based on the extensive understanding of the biochemical interactions between OPs and AChE, the relationship between OP activation and detoxification is of critical importance in determining the toxicological response to OP insecticides (Ma and Chamber, 1984). In this regard, Gearhart *et al*. (1990) suggested that physiologically based pharmacokinetic and pharmacodynamic (PBPK/PD) models capable of predicting the relationship between OP exposure and AChE inhibition are useful for evaluating the risk associated with a given OP exposure. Although a limited number of PBPK/PD models for OP insecticides and nerve agents have been published in the literature (Abbas and Hayton, 1997; Gearhart *et al*., 1990; Maxwell *et al*, 1988; Sultatos, 1990), there are currently no models for the phosphorothionate insecticide CPF.

The primary objective of the research reported herein was to develop and validate a PBPK/PD model for CPF in rats and humans. This model quantitatively integrates target tissue dosimetry and dynamic response describing the pharmacokinetics of CPF, CPF-oxon, and TCP, as well as the associated cholinesterase (ChE) inhibition kinetics in blood components (plasma and red blood cell (RBC)) and selected tissues, including the brain. To develop and validate the model, pharmacokinetic/pharmacodynamic studies were conducted in both rats and humans to quantitate dosimetry and dynamic response over a range of CPF doses. In addition, the model was further evaluated against available dosimetry and dynamic response data in the published literature.

MATERIALS AND METHODS

Chemicals. Chlorpyrifos was obtained from Dow AgroSciences (Indianapolis, IN) and had a chemical purity of 99.8%. $^{13}C_2$-^{15}N-Chlorpyrifos, $^{13}C_2$-^{15}N-chlorpyrifos-oxon, and $^{13}C_2$-trichloropyridinol were utilized as internal standards for the negative-ion chemical ionization, gas chromatography–mass spectrometry (NCI/GC/MS) for CPF, CPF-oxon, and TCP, respectively.

Animals. Male Fischer 344 (F344) rats (Charles River Laboratories Inc., Raleigh, NC) were utilized for the pharmacokinetic/pharmacodynamic studies (time points, 10 min–12 h postdosing) and were 10–11 weeks of age at the time of dosing. Female F344 rats were purchased from the same supplier and were also utilized to assess the pharmacodynamic response (time point, 24 h postdosing) and were ~7 weeks of age at the start of the study. Animals were housed one per cage (wire mesh or plastic), and maintained on a 12-h photocycle, at controlled temperature (22–24°C), and relative humidity (44–52%) and allowed access to municipal tap water and Purina certified rodent chow *ad libitum*, except where otherwise noted.

Model structure. A diagram of the PBPK/PD model structure developed for CFP and CPF-oxon is illustrated in Figure 1 and is based on the model for diisopropylflurophosphate (DFP) in rats (Gearhart *et al.*, 1990). The current PBPK/PD model was developed to describe the time course of absorption, distribution, metabolism, and excretion of CPF, CPF-oxon, and TCP, and the inhibition of target esterases by CPF-oxon in the rat and human. The model assumes that the pharmacokinetic and pharmacodynamic response in rats and humans is independent of gender, which is consistent with the observed response in human males and females reported in this study. The absorption of CPF following oral administration in corn oil vehicle required the use of a two-compartment uptake model to simulate absorption, according to Staats *et al*. (1991). This two-compartment model incorporated 1st-order rate equations to describe systemic uptake and transfer between compartments. In addition, absorption of CPF from the diet was incorporated into the model to allow for the simulation of chronic dietary administration. In the chronic dietary studies with CPF, the doses (mg/kg/day) determined were based upon the measured rate of food consumption per day. To model the data, the absorbed dose was expressed as a constant zero-order rate (mg/h) over a 12-h interval. This assumption was reasonable since, in rats, the majority of the daily food intake occurs during the lights-off cycle (~12 h) (Jochemsen *et al*., 1993). Equations to describe the dermal uptake of CPF into the skin compartment of humans were adapted from Poet *et al.* (2000). In this model, physiological and metabolic parameters (i.e., tissue volume, blood flow, and metabolic capacity) were scaled as a function of body weight, according to the methods of Ramsey and Andersen (1984). The CYP450-mediated activation and detoxification of CPF to CPF-oxon and TCP, respectively, was limited to the liver compartment. The model was linked to the CPF-oxon model that contained equations to describe the A-EST hydrolysis of CPF-oxon to TCP in both the liver and blood compartments. The CYP450 activation/detoxification and A-EST detoxification of CPF-oxon were all described as Michaelis-Menten processes. Interactions of the oxon with B-EST (AChE, BuChE, and CaE) were modeled as 2nd-order processes occurring in the liver, blood (plasma and RBC), brain, and diaphragm. The B-EST enzyme levels (μmol) in blood, brain, liver, and diaphragm were calculated based on the enzyme turnover rates and enzyme activities reported by Maxwell *et. al.* (1987), and these were based on a balance between basal degradation and enzyme resynthesis. Following exposure to CPF-oxon, the amount of available B-EST was determined by finding a balance between the bimolecular rate of inhibition and the rate of B-EST regeneration (reactivation and resynthesis). In this model, TCP was formed by the direct CYP450 metabolic conversion of CPF and through A-EST-mediated hydrolysis of CPF-oxon and B-EST binding of CPF-oxon, respectively. The blood kinetics and urinary elimination of TCP were described with a simple one-compartment model utilizing a 1st-order rate of urinary elimination.

Model parameters. To develop this model, several types of data were required, including physiological constants, partition coefficients, and biochemical constants describing the metabolism of CPF, CPF-oxon, and the inhibition of B-EST by CPF-oxon. These data were obtained from the literature, from experimentation, or by optimization of model output utilizing the computer simulation. The PBPK/PD model code for simultaneous solution of both algebraic and differential equations was developed in SIMUSOLV®, a computer program containing a numerical integration, optimization, and graphical routine, and is based on the Fortran-based software ACSL. The values, assumptions, and references used for these parameters are listed in Tables 1 and 2.

Physiological constants and partition coefficients. Organ volumes, cardiac output, and tissue blood flows were adapted from the DFP model developed by Gearheart *et al*. (1990) or obtained from the literature (Brown *et al*., 1997). The partitioning coefficients for CPF and CPF-oxon were estimated, based on their octanol:water partitioning coefficients and tissue lipid content based on an algorithm developed by Poulin and Krishnan (1995).

Biochemical constants. The metabolism of CPF to TCP and CPF-oxon is mediated by CYP450 and is described using Michaelis-Menten kinetics. A range of K_m and V_{max} parameters has been determined *in vitro*, utilizing tissue obtained from both mice and rats (Ma and Chambers, 1994, 1995; Mortensen *et al*., 1996; Pond *et al*., 1995; Sultatos and Murphy, 1983; Sultatos *et al*., 1984). The selection of a reasonable set of model parameters was determined by evaluating the overall goodness of fit of the model against the experimental data over the range of reported rate constants for enzyme affinity and activities. Sultatos *et al.* (1984) previously reported that CPF was extensively bound (~97%) to plasma proteins over a broad range of concentrations. It was also assumed that CPF-oxon would exhibit an even higher plasma protein binding based upon oxon reactivity, although the extent of CPF-oxon plasma protein binding has not yet been experimentally determined. In the current model structure, the total amount of absorbed CPF is directly added to the liver compartment. However, once in the systemic circulation, only nonbound (i.e.,

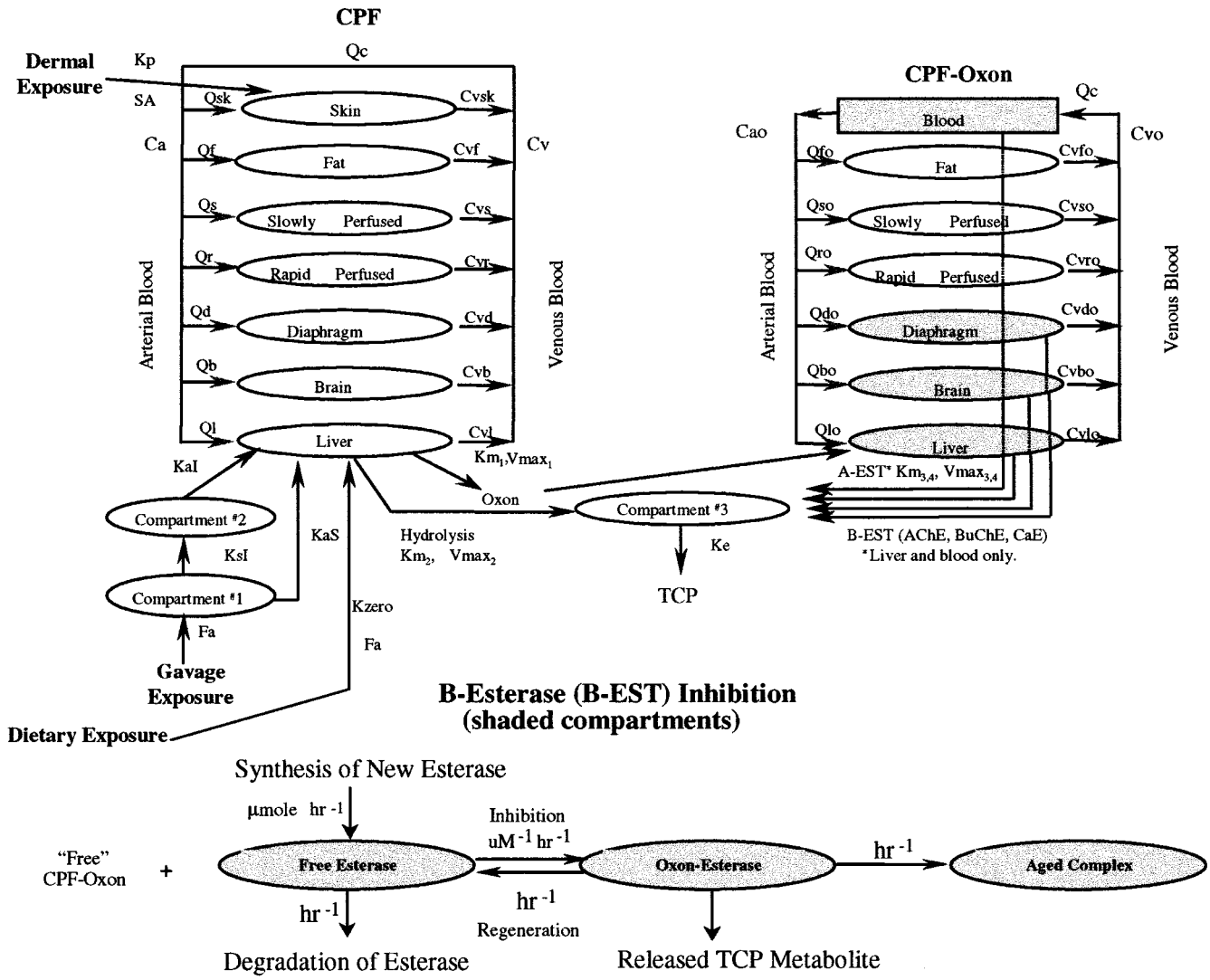

FIG. 1. Physiologically based pharmacokinetic and pharmacodynamic model used to describe the disposition of chlorpyrifos (CPF), CPF-oxon, and trichloropyridinol (TCP), and B-esterase (B-EST) inhibition in rats and humans following oral (gavage, dietary) and dermal exposure to CPF. The shaded tissue compartments indicate organs in which B-EST (AChE, BuChE and CaE) enzyme activity is described. Model parameter definitions: QC, cardiac output (l/h); Q_i, blood flow to "i" tissue (l/h); Ca, arterial blood concentration of CPF (μmol/l); Cao, arterial blood concentration of CPF-oxon (μmol/l); Cv, pooled venous blood concentration of CPF (μmol/l); Cvo, pooled venous blood concentration of CPF-oxon (μmol/l); Cv_i, venous blood concentration of CPF draining "i" tissue (μmol/l); Cv_io, venous blood concentration of CPF-oxon draining "i" tissue (μmol/l); SA, surface area of skin exposed (cm^2); KP, skin permeability coefficient (cm/h); K_{zero}, zero (μmol/h) rate of absorption of CPF from diet; Fa fractional absorption (%) gavage dose; KaS and KaI, 1st-order rate constant for absorption of CPF from compartments 1 and 2 (per h); KsI, 1st-order rate constant for transfer of CPF from compartments 1 and 2 (per h); Ke, 1st-order rate constant for elimination of TCP from compartment 3; Km_{1-4}, Michaelis constant for saturable process (μmol/l); $Vmax_{(1-4)}$, maximum velocity for saturable process (μmol/h).

free) parent chemical or metabolite was capable of entering the tissue compartments.

B-esterase (B-EST) inhibition. The model structure for the inhibition of B-EST (AChE, BuChE, and CaE) by CPF-oxon in plasma, RBC, diaphragm, and liver were likewise based on the model structure developed by Gearhart *et al.* (1990). However, when available, CPF-specific model parameters for bimolecular inhibition (Ki), reactivation (Kr), and aging (Ka) were incorporated into the model (Amitai *et al.*, 1998; Carr and Chambers, 1996). Reactivation and aging rates were not available for CPF-oxon inhibition of BuChE or CaE so these parameters were set at the rates for CPF-oxon interaction with AChE. The amount of enzyme (μmol), zero-order synthesis rate (μmol/h), and 1st-order degradation rate (h^{-1}) of AChE, BuChE, and CaE for each of the tissue compartments was calculated as previously described (Gearhart *et al.* 1990; Maxwell *et al.* 1987). The CaE enzyme degradation rate (Kd) and Ki constants were estimated for each tissue by fitting the model to data obtained by Chanda *et al.* (1997). The Ki parameters for AChE and BuChE blood and tissue activity were estimated by fitting the experimental data from Figure 2. The esterase recovery rates in the various tissue compartments were obtained from a previous study (Gearhart *et al.*, 1990) or by fitting the oral dose plasma BuChE data from Nolan *et al.* (1984).

In light of the importance of RBC AChE inhibition as a biomarker for OP insecticide exposure, RBC AChE inhibition was incorporated into the PBPK/PD model structure. The total amount of available RBC AChE (μmol) in the rat was calculated based on the experimentally determined total RBC

TABLE 1

Parameters used in the Physiologically Based Pharmacokinetic Model for CPF and CPF-oxon to Describe Dosimetry and Metabolism

Parameter	Rat	Human	Estimation method[a]
Percentage of body weight			
Blood	6	7	Fixed[b,c]
Brain	1.2	2	Fixed[b,c]
Diaphragm	0.03	0.03	Fixed[b,c]
Fat	7	21	Fixed[b,c]
Liver	4	3	Fixed[b,c]
Rapidly perfused	4	4	Fixed[b,c]
Slowly perfused	78	63	Fixed[b,c]
Flows (l/h)			
Cardiac output	5.4	347.9	Fixed[d]
% cardiac output			
Brain	3	11.4	Fixed[b,c]
Diaphragm	0.6	0.6	Fixed[b,c]
Fat	9	5.2	Fixed[b,c]
Liver	25	23	Fixed[b,c]
Rapidly perfused	42.6	40	Fixed[b,c]
Slowly perfused	14	14	Fixed[b,c]
Skin	5.8	5.8	Fixed[c]
Partition coefficients for CPF			
Brain/blood	33	33	Calculated[e]
Diaphragm/blood	6	6	Calculated[e]
Fat/blood	435	435	Calculated[e]
Liver/blood	22	22	Calculated[e]
Rapidly perfused/blood	10	10	Calculated[e]
Slowly perfused/blood	6	6	Calculated[e]
Skin/blood	6	6	Calculated[e]
Partition coefficients for CPF-oxon			
Brain/blood	26	26	Calculated[e]
Diaphragm/blood	4.9	4.9	Calculated[e]
Fat/blood	342	342	Calculated[e]
Liver/blood	17	17	Calculated[e]
Rapidly perfused blood	8.1	8.1	Calculated[e]
Slowly perfused blood	4.9	4.9	Calculated[e]
Metabolic constants			
CYP450 CPF-to- oxon (liver)			
Km_1 (μmol/l)	2.86	2.86	Fixed[f]
$VmaxC_1$ (μmol/h/kg)	80	80	Fixed[f]
CYP450 CPF-to-TCP			
Km_2 (μmol/l)	24	24	Fixed[f]
$VmaxC_2$ (μmol/h/kg)	273	273	Fixed[f]
A-EST oxon-to-TCP (liver)			
Km_3 (μmole/l)	240	240	Fixed[g]
$VmaxC_3$ (μmole/h/kg)	74421	74421	Fixed[g]
A-EST oxon-to-TCP (blood)			
Km_4 (μmol/l)	250	250	Fixed[g]
$VmaxC_4$ (μmol/h/kg)	57003	57003	Fixed[g]
Oral absorption parameters			
KaS (stomach; hr^{-1})	0.01	0.01	Fitted[k]
KaI (intestine; hr^{-1})	0.5	0.5	Fitted[k]
KsI (transfer stomach-intestine/h)	0.5	0.5	Fitted[k]
Fa (fractional absorption; %)	0.80	0.72	Fixed[h]
Dermal absorption parameter			
Surface area (cm^2)	—	100	Fixed[i]
Kp (permeability coefficient; cm/h)	—	4.81 E^{-5}	Fitted[h]
TCP model parameters			
Vd (l)	35	35	Fitted[h]
Ke (per h)	0.017	0.017	Fitted[h]
Plasma protein binding			
CPF (%)	97	97	Fixed[j]
CPF-oxon (%)	98	98	Fixed[j]

[a]The model parameters were estimated independently and held fixed (fixed), measured in independent experiments (measured), calculated utilizing mathematical algorithms (calculated) or estimated by fitting the model to the data (fitted). Dash indicates that the parameter was not incorporated into the model.

[b]Gearhart *et al*., 1990 (rat).

Brown *et al.*, 1997 (human).

[d]Andersen *et al*., 1987.

[e]Poulin and Krishnan, 1995.

AChE enzyme activity in control animals. The Ki rate constant for RBC inhibition was initially obtained from the literature (Amitai *et al*., 1998), and the recovery of RBC AChE enzyme was based on the rate of RBC replenishment, assuming a RBC lifespan of 50 and 122 days in the rat and human, respectively (Schalm, 1961). Initial RBC AChE inhibition simulations in the rat had a slower enzyme recovery, when compared against the results from a previously published study (Nostrandt *et al*., 1997). Since RBC AChE resynthesis was assumed to be primarily the result of new RBC formation, a slightly faster reactivation rate (see Table 2) was required to account for the recovery of RBC AChE activity observed 24 h postdosing.

Pharmacokinetic/Pharmacodynamic Studies

To develop and validate the CPF PBPK/PD model, pharmacokinetic/pharmacodynamic studies were conducted in both rats and humans.

Rat. The time course of CPF and CPF-oxon in the blood and the activity of ChE in the plasma, and AChE in brains of male (F344) rats were determined following oral administration of 100, 50, 10, 5, 1, and 0.5 mg CPF/kg of body weight. An additional group of female rats were administered the same doses of CPF and plasma; RBC, and selected tissue ChE activity was determined at 24 h postdosing. The dose solution was prepared in a corn oil vehicle and administered by gavage, and all animals were fasted for approximately 16 h prior to administration of CPF. Four animals per time point were humanely anesthetized, sacrificed, and tissues were collected at 10 and 20 min, and 1, 3, 6, 12, and 24 h postdosing for CPF, CPF-oxon, or ChE analysis. The blood was collected, via cardiac puncture, into heparinized syringes containing an acidic salt solution (2.5 N acetic acid/saturated sodium chloride), which effectively halted the enzymatic hydrolysis of CPF-oxon. These specimens were then analyzed for the presence of CPF and CPF-oxon by NCI-GC-MS as described by Brzak *et al*. (1998). The limit of quantitation (LOQ) for both CPF and CPF-oxon was determined to be 3 nmol/l of blood. An additional blood sample was collected at each time point, and centrifuged to separate the plasma and RBC (24 h postdosing only) for analysis of plasma ChE and RBC AChE activity. In addition, brains were removed, rapidly frozen by submersion in liquid nitrogen, and both the plasma and brains were then stored at −80°C until assayed for esterase activity. Brain and RBC AChE, and plasma ChE activity assays were performed with Boehringer Mannheim (Indianapolis, IN) reagents on a Hitachi 914 clinical chemistry analyzer utilizing acetylthiocholine (AcTh) as an enzyme substrate, as previously described (Ellman *et al*., 1961).

Human volunteer pharmacokinetic study. A double-blind, placebo-controlled clinical pharmacokinetic study was conducted at MDS Harris Laboratory (Lincoln, NE), in accordance with all applicable U.S. guidelines as specified in Title 21 of the Code of Federal Regulations (parts 50, 56 and 321) and the International Guidelines for Human Testing as promulgated in the Declaration of Helsinki (1964; amended 1996). The overall objective of this study was to provide needed data to better define the pharmacokinetics of CPF in humans. In this study, groups of 6 male and 6 female volunteers received a single oral dose of 0, 0.5, 1, or 2 mg CPF/kg of body weight in capsule form. The volunteers were confined to the testing facility for the first 24-h posttreatment period, and their health status was closely monitored during this time, providing a mechanism to confirm the presence or absence of cholinergic or other treatment-related effects. After the initial 24-h interval, the volunteers were allowed to go home but continued to return to the testing facility for the collection of additional blood specimens. Blood was collected at each interval by venipuncture and the targeted collection intervals were 2, 4, 8, 12, 24, 36,

[f]Ma and Chambers, 1994.

[g]Mortensen *et al.*, 1996.

[h]Nolan *et al.*, 1984 (human); Dow, unpublished data (rat).

[i]McDougal *et al*., 1986.

[j]Sultatos *et al*., 1984 (data only available for CPF; model assumes binding is slightly higher for CPF-oxon).

[k]Estimated by fitting model to data from Figure 2.

TABLE 2
Parameters Used in the Pharmacodynamic Model for CPF-oxon Inhibition of AChE, BuChE and CaE

Parameter	Rat	Human	Estimation Method[a]
Enzyme Turnover Rate (Enz. Hydro./hr^{-1})			
AChE	1.17 E^{+7}	1.17 E^{+7}	Fixed[b]
BuChE	3.66 E^{+6}	3.66 E^{+6}	Fixed[b]
CaE	1.09 E^{+5}	1.09 E^{+5}	Fixed[b]
Enzyme Activity (μmole/kg/hr^{-1})			
Brain AChE	4.4 E^{+5}	4.4 E^{+5}	Fixed[b]
Diaphragm AChE	7.74 E^{+4}	7.74 E^{+4}	Fixed[b]
Liver AChE	1.02 E^{+4}	1.02 E^{+4}	Fixed[b]
Plasma AChE	1.32 E^{+4}	—	Fixed[b]
Brain BuChE	4.68 E^{+4}	4.68 E^{+4}	Fixed[b]
Diaphragm BuChE	2.64 E^{+4}	2.64 E^{+4}	Fixed[b]
Liver BuChE	3.0 E^{+4}	3.0 E^{+4}	Fixed[b]
Plasma BuChE	1.56 E^{+4}	1.73 E^{+6}	Fixed[b]/Fitted[g]
Brain CaE	6.0 E^{+3}	6.0 E^{+3}	Fixed[b]
Diaphragm CaE	3.18 E^{+5}	3.18 E^{+5}	Fixed[b]
Liver CaE	1.94 E^{+6}	1.94 E^{+6}	Fixed[b]
Plasma CaE	4.56 E^{+5}	4.56 E^{+5}	Fixed[b]
Enzyme Degradation Rate (hr^{-1})			
Kd_1 Brain AChE	0.01	0.01	Fixed[c]
Kd_2 Diaphragm AChE	0.01	0.01	Fixed[c]
Kd_3 Liver AChE	0.1	0.1	Fixed[c]
Kd_4 Plasma AChE	0.1	—	Fixed[c]
Kd_5 RBC AChE	0.008	0.0008	Fixed[j]
Kd_6 Brain BuChE	0.01	0.01	Fixed[c]
Kd_7 Diaphragm BuChE	0.01	0.01	Fixed[c]
Kd_8 Liver BuChE	0.1	0.1	Fixed[c]
Kd_9 Plasma BuChE	0.1	4.2 E^{-3}	Fixed[c]/Fitted
Kd_{10} Brain CaE	7.54 E^{-4}	7.54 E^{-4}	Fitted[f]
Kd_{11} Diaphragm CaE	0.001	0.001	Fitted[f]
Kd_{12} Liver CaE	0.001	0.001	Fitted[f]
Kd_{13} Plasma CaE	0.0033	0.0033	Fitted[f]
Bimolecular Inhibition Rate (μM hr)$^{-1}$			
$Ki_{1\text{-}4}$ All Tissues AChE	243	243	Fitted[e]
Ki_5 RBC AChE	100	100	Fitted[i]
$Ki_{6\text{-}9}$ All Tissues BuChE	2000	2000	Fitted[f]
Ki_{10} Brain CaE	20	20	Fitted[f]
Ki_{11} Diaphragm CaE	20	20	Fitted[f]
Ki_{12} Liver CaE	20	20	Fitted[f]
Ki_{13} Plasma CaE	20	20	Fitted[f]
Reactivation Rate (hr^{-1})			
$Kr_{1\text{-}4}$ AChE	1.43 E^{-2}	1.43 E^{-2}	Fixed[d]
Kr_5 RBC AChE	4.0 E^{-2}	4.0 E^{-2}	Fitted[k]
$Kr_{6\text{-}9}$ BuChE	1.43 E^{-2}	1.43 E^{-3}	Fixed[d]/Fitted[l]
$Kr_{10\text{-}13}$ CaE	1.43 E^{-2}	1.43 E^{-2}	Fixed[d]
Aging Rate (hr^{-1})			
$Ka_{1\text{-}5}$ AChE	1.13 E^{-2}	1.13 E^{-2}	Fixed[d]
$Ka_{6\text{-}9}$ BuChE	1.13 E^{-2}	1.13 E^{-2}	Fixed[d]
$Ka_{10\text{-}13}$ CaE	1.13 E^{-2}	1.13 E^{-2}	Fixed[d]
RBC life-span (days)	50	122	Fixed[h]

[a]The model parameters were estimated independently and held fixed (fixed), measured in independent experiments (measured), or estimated by fitting the model to the data (fitted). Dash indicates that the parameter was not incorporated into the model.
[b]Maxwell *et al.* 1987.
[c]Gearhart *et al*. 1990, (rat).
[d]Carr and Chambers 1996.
[e]Estimated by fitting model to data from Figure 4.
[f]Estimated by fitting model to data on CaE inhibition from Chanda *et al.*, 1997.
[g]Estimated by fitting model to data from Figure 8.
[h]Schalm 1961.
[i]Estimated by fitting model to data from Figure 10.
[j]Estimated based on RBC life-span.
[k]Estimated by fitting model to Zheng *et al*., 2000 and data from Table 4.
[l]Estimated by fitting model to human oral data in Figure 7.

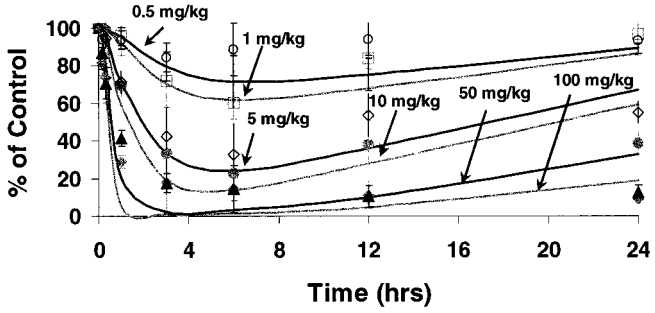

FIG. 2. Experimental data (symbols) and simulations (lines) for the inhibition of plasma ChE in F344 rats administered CPF by oral gavage at dose levels of 0.5 (open circle), 1 (open square), 5 (open diamond), 10 (filled circle), 50 (filled triangle) and 100 mg/kg (filled diamond). The data represent the mean ± SD of 4 animals per treatment group. (Note: the data through 12 h postdosing was obtained in male rats, whereas the 24 h postdosing data point was obtained in females).

48, 72, 96, 120, 144, and 168 h following treatment. In addition to blood, urine specimens were collected prior to treatment and through 168 h postdosing. Blood and urine specimens were analyzed for the presence of CPF, CPF-oxon, and TCP by GC-NCI-MS (Brzak *et al*., 1998). The LOQ for CPF and CPF-oxon in blood was 3 nmol/l, whereas the TCP LOQ was determined to be 50 nmol/l. In urine specimens, the LOQ for CPF and CPF-oxon was 3 or 3.5 nmol/l and 1 nmol/l for TCP. In addition, blood specimens were centrifuged to separate plasma from RBC and the inhibition of RBC AChE was determined as previously described (Ellman *et al*., 1961). The area-under-the-concentration curve ($AUC_{0-\alpha}$) for blood and urinary TCP excretion were determined using the trapezoidal rule (Renwick, 1994) and the extent of absorption was calculated based on the amount of TCP recovered in the urine, as described by Nolan *et al.* (1984).

RESULTS

Pharmacokinetics/pharmacodynamics of CPF in the rat. All animals survived the single acute oral administration of CPF at doses ranging from 0.5 to 100 mg/kg, and the time course of CPF in the blood and model prediction is presented in Figure 3. CPF was quantifiable at all 6 time points, only for those animals administered the 100 mg/kg dose, while none of the blood samples from the 0.5-mg/kg treatment group had quantifiable levels of CPF. This limited kinetic data suggests that CPF was rapidly absorbed and metabolized with peak blood levels being observed by 3 h postdosing. The blood-CPF $AUC_{0-\alpha}$ was calculated as 0.4, 1.1, 5.0, and 12.5 μmol/h/l and was essentially proportional to dose at all levels. However, at the highest dose tested (100 mg/kg), there was a small deviation from proportionality that was primarily associated with a slightly higher observed blood concentration of CPF at 12 h postdosing. The limited number of quantifiable blood samples over the dose range evaluated made it difficult to adequately model these data. Initially, CPF uptake was modeled utilizing a single 1st-order process, which resulted in a much more rapid rise to peak concentrations than the data suggested. Therefore, to better describe the absorption of CPF following oral administration from a corn oil vehicle, a two-compartment gastroin-

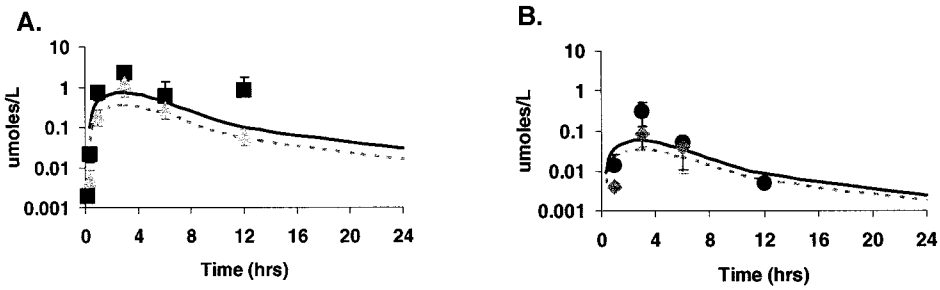

FIG. 3. Experimental data (symbols) and simulations (lines) for the concentration of CPF in the blood of F344 rats administered CPF by oral gavage at dose levels of (A) 50 (triangle) and 100 mg/kg (square), (B) 5 (diamond), and 10 mg/kg (circle). The data represent the mean ± SD of 4 animals per treatment group.

testinal (GI) tract model was utilized as previously described (Staats *et al*., 1991). Although this clearly improved the overall fit, the model did underestimate the peak (3 h) blood CPF concentration for all treatment groups. Blood specimens were also analyzed for the presence of CPF-oxon, which was only detectable in a few of the samples obtained from rats administered doses greater than 10 mg/kg. In general, the concentration of CPF-oxon in the blood, when detectable, had a concentration that ranged from 2–7 nmol/l (data not shown) which is ~50–140× less than the observed CPF concentration in these same samples (100–1000 nmol/l). Although it was feasible to identify CPF-oxon in the blood, the observed results were very close to the analytical limits of quantitation, which likely contributed to the highly variable response observed. This variable response and the limited number of quantifiable samples made it particularly difficult to adequately model the CPF-oxon pharmacokinetics. However, over the dose range evaluated, the model predicted that the observed CPF-oxon concentrations ranged from 3 to 36 nmol/l blood (data not shown), which, although slightly higher than the measured concentrations, were reasonably comparative given the limitations of the data.

To adequately describe the CPF-oxon stoichiometric inhibition of both target (i.e., AChE) and nontarget B-EST (i.e., BuChE, and CaE), the amount of CaE, BuChE, and AChE were calculated for the liver, plasma, RBC, brain, and diaphragm compartments (See Fig. 1). As previously noted, the total number of available B-EST binding sites in the various tissues were based on a previous study conducted in rats (Maxwell *et al.*, 1987). The authors reported an overall tissue B-EST ratio of AChE:BuChE:CaE to be 1:2:2051, which indicates that the overall number of CaE binding sites far exceeds the number of sites available for either AChE or BuChE binding in the rat. However, Maxwell *et al*. (1987) also noted that between tissues there were clear differences in the distribution of B-EST enzymes. Although the plasma ChE in rat contains appreciable amounts of both AChE and BuChE (ORNL, 2000), in humans the plasma is devoid of AChE enzyme (Ecobichon and Comeau, 1973); therefore, only BuChE and CaE enzyme activity were incorporated into the PBPK/PD model describing the plasma esterase in humans. Although reasonable initial parameters were obtainable from the literature for CPF-oxon inhibition of AChE and BuChE, experimentally determined parameters were not available for CPF-oxon inhibition of CaE. To address this deficiency the AChE model parameters were utilized as a starting point. It has previously been demonstrated that the sensitivity of esterases to OP inhibition, based on experimentally determined Ki values for DFP, followed the order: BuChE >> AChE > CaE (Gearhart *et al*., 1990). Similarly, Amitai *et al*. (1998) reported that CPF-oxon had a much larger Ki for BuChE than AChE in both rodents and humans (Ki ~100,000 and 581 μM/h, respectively). Since a Ki for CaE inhibition was not available for CPF-oxon, an apparent Ki was estimated to be 20 μM/h based on the ratio of Ki's for AChE and CaE reported by Gearhart *et al.* (1990). Hence, for all model simulations the Ki for CaE inhibition was held constant at 20 μM/h, and only the enzyme degradation rates (Kd) were optimized to fit the CaE inhibition data reported by Chanda *et al.* (1997). The CaE model parameters were then held constant for all remaining model simulations (data not shown).

The time course of plasma ChE and brain AChE inhibition were also determined in rats through 24 h of postdosing following single oral gavage administration of CPF at doses ranging from 0.5 to 100 mg/kg, and the experimental results and model simulations are illustrated in Figures 2 and 4. In these experiments, CPF produced a dose-dependent reduction in both plasma ChE and brain AChE activity. As might be expected at any given dose, plasma esterase was inhibited to a greater extent than brain. The maximum inhibition of plasma

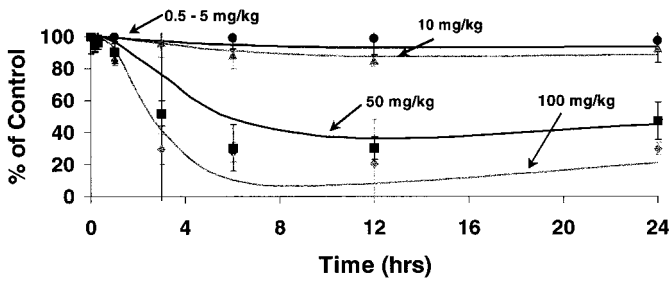

FIG. 4. Experimental data (symbols) and simulations (lines) for the inhibition of brain AChE in F344 rats administered CPF by oral gavage at dose levels of 0.5–5 (filled circle), 10 (filled triangle) 50 (filled square) and 100 mg/kg (filled diamond). The data represent the mean ± SD of 4 animals per treatment group. (Note: the data through 12 h postdosing was obtained in male rats, whereas, the 24 h postdosing data point was obtained in females)

TABLE 3
Experimental Data (Observed) and Simulations (Predicted) for Red Blood Cell Acetylcholinesterase (RBC AChE) Measured at 4 and 24 h Postdosing following Oral Administration in Sprague-Dawley and F344 Rats

Dose (mg/kg)	4 h Postdosing			24 h Postdosing		
	% Control		Ratio predicted/ observed	% Control		Ratio predicted/ observed
	Observed	Predicted		Observed	Predicted	
0.15	100	98.8	0.98	ND	ND	—
0.45	100	96.5	0.97	ND	ND	—
0.75	100	94.1	0.94	102.9 ± 10.87	95.8	0.93
1	ND	ND	—	97.3 ± 8.87	91.8	0.94
1.5	68	88.6	1.30	ND	ND	—
4.5	54	69.7	1.29	ND	ND	—
5	ND	ND	—	82.8 ± 12.0	69.2	0.84
7.5	27	54.9	2.03	ND	ND	—
10	ND	ND	—	70.7 ± 10.0	54.2	0.77
15	15	31.0	2.07	ND	ND	—
50	ND	ND	—	48.1 ± 9.01	26.1	0.54
100	ND	ND	—	49.2 ± 8.8	16.8	0.34

Note. ND, not determined; 4-h postdosing data extracted from Zheng *et al.*, 2000; 24-h postdosing data determined experimentally; $n = 6$ animals/treatment group. Experimentally determined data are given as mean ± SD.

ChE was observed at 3 to 6 h after the 0.5 to 10 mg/kg doses, and 3 to 12 h after the 50 and 100 mg/kg doses; doses of 50 mg/kg or greater resulted in a maximum inhibition of plasma ChE (~90%). Inhibition of brain AChE occurred at dose levels of 10 mg/kg and higher. Maximum inhibition of brain AChE occurred from 6 to 12 h postdosing at doses of 10 and 50 mg/kg, and at 3 to 12 h after the 100-mg/kg dose.

The DFP PBPK/PD model developed by Gearhart *et al.* (1990) estimated the rate of plasma ChE and brain AChE synthesis and degradation by model optimization against DFP experimental data sets, and their optimum Kd's ranged from 0.01 to 0.1 per h in mice and rats. These synthesis and degradation parameter estimates were likewise used in the current model. Amitai *et al.* (1998) determined the *in vitro* Ki value for CPF-oxon binding kinetics with purified AChE and BuChE enzymes to be ~48,000, 471, and 228 (μM/h) for plasma BuChE, plasma AChE, and RBC AChE, respectively. However, utilizing these Ki parameters in the model overestimated the extent of plasma BuChE and AChE inhibition kinetics (data not shown); therefore, the *in vitro* Ki's were reduced to an apparent *in vivo* Ki to better describe the data (see Table 2). By establishing an apparent Ki for BuChE and AChE enzyme activity, the PBPK/PD model reasonably simulated the dose-dependent inhibition of both the plasma ChE and brain AChE inhibition kinetics over the broad dose range evaluated through 24 h postdosing. The model accurately reflected the overall trends associated with plasma ChE and brain AChE inhibition kinetics in the rat, and in particular reflected the large increase in enzyme inhibition at doses of 5 and 50 mg/kg in the plasma and brain, respectively.

The extent of RBC AChE inhibition was likewise determined at 24 h postdosing in rats orally administered CPF at single doses ranging from 0.5 to 100 mg/kg. In addition, single dose RBC AChE inhibition data (4 h postdosing) at doses ranging from 0.15 to 15 mg/kg was obtained from Zheng *et al.* (2000). The resulting inhibition and model-simulated prediction of the enzyme inhibition at 4 and 24 h postdosing are presented in Table 3. The inhibition of the RBC AChE activity was dose-dependent; however the RBC's were less sensitive to inhibition than plasma ChE, and a no-effect level was seen at doses of 1 mg/kg or less. The apparent Ki for the RBC's was less than for plasma AChE (~100 vs. 243 μM/h, respectively), and the reactivation rate (Kr) was set at 0.04/h to accommodate a faster reactivation, through 24 h postdosing, that could not be accounted for by RBC resynthesis alone. With these parameters, the model dose response was consistent with the experimental data, although the model slightly underpredicted the peak 4-h inhibition (pred/obs ratios 0.94–2.07), while slightly overpredicting the 24 h postdosing data (pred/obs ratios 0.34–0.94). Overall, the model predictions were generally within a factor of 2 of the experimental data.

Model predictions of effects of repeated dietary doses on CPF in the rat. The PBPK/PD rat model was developed from literature citations and from fitting the data from single-dose studies. The unaltered model was used to predict the effects of repeated daily exposure to CPF in the diet. Since the majority of long-term toxicity testing with CPF has been conducted by continuously exposing rodents to CPF via the diet, the model incorporated a dietary exposure regimen. The results of the

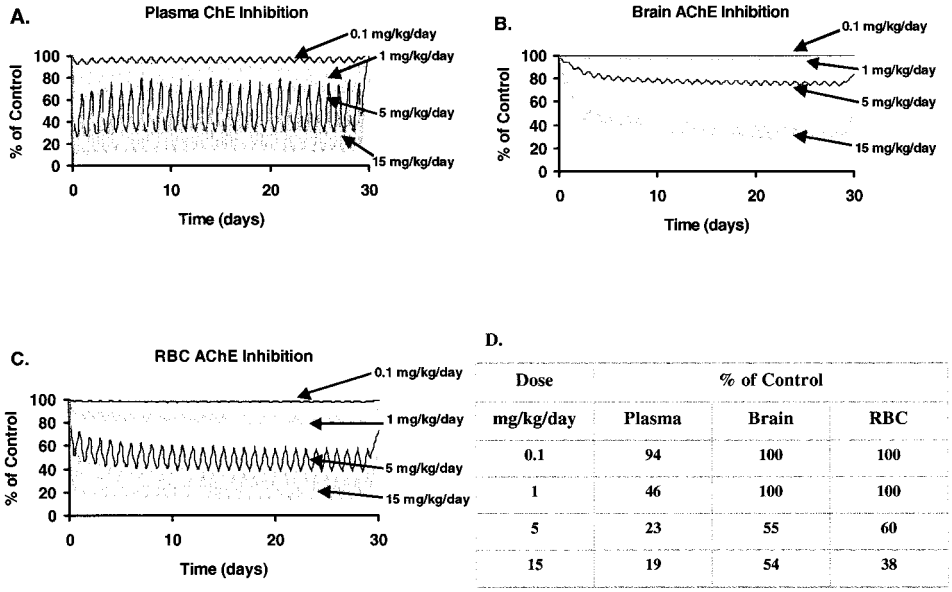

D.

Dose	% of Control		
mg/kg/day	Plasma	Brain	RBC
0.1	94	100	100
1	46	100	100
5	23	55	60
15	19	54	38

FIG. 5. Model simulation of ChE inhibition in plasma (A), brain AChE (B), and RBC AChE (C) in F344 rats following dietary administration of CPF for ~30 days at doses of 0.1, 1, 5, and 15 mg/kg/day. The plasma, RBC and brain table insert (D) represents experimental data from Yano *et al.* (2000), obtained following 7 to 13 weeks of repeated dietary exposure to CPF.

repeated CPF dietary dosing model simulations on rat brain AChE, RBC AChE, and plasma ChE inhibition in comparison to experimental results obtained following 7 to 13 weeks of dietary CPF administration (Yano *et al.*, 2000) are presented in Figure 5. The model simulation suggested that a steady-state level of enzyme inhibition was rapidly attained by 3 to 4 days following initiation of dosing, although the brain AChE inhibition at the highest dose (15 mg/kg/day) appears to continue to decline through 30 days of exposure. The model also indicated a dose-dependent inhibition in all tissues with the order of magnitude of inhibition as follows: plasma > RBC > brain. Following a 0.1 mg/kg/day dose of CPF, the PBPK/PD model accurately described the lack of brain (100% of control), and RBC AChE inhibition (~98% of control) and minimal plasma ChE inhibition (~96% of control). The model also predicted the lack of brain AChE inhibition (100% of control) and slight RBC AChE inhibition (~80% of control) following exposure to a 1 mg CPF/kg/day dose. However, the model underestimated the extent of plasma ChE (~75% of control) inhibition relative to the experimental results (46% of control). Simulating a continuous dose of 5 mg/kg/day, the model also underpredicted the plasma ChE (~50% vs. 23% of control), and brain AChE inhibition kinetics (~80% vs. 55% of control) relative to the experimental data, but reasonably estimated RBC AChE (~50% vs. 55% of control) inhibition. Finally, following a repeated dietary exposure to 15 mg CPF/kg/day, the model reasonably estimated the extent of plasma ChE (~25% vs. 19% of control), brain AChE (~38% vs. 54% of control), and RBC AChE inhibition (~30% vs. 38% of control) kinetics. The model response suggested that, at doses ≥ 5 mg CPF/kg/day, the CPF-oxon concentration in the brain attained an adequate concentration to overwhelm available detoxification pathways resulting in significant brain AChE inhibition. The experimental data of Yano *et al.* (2000) is consistent with the model simulations, but slight quantitative differences suggest that detoxification pathways may be overwhelmed at lower doses (i.e., between 1 and 5 mg/kg/day) than the current PBPK/PD model predicts. It is conceivable that matrix effects associated with corn oil vs. dietary dose preparation and administration could result in variable oral bioavailability, which would effectively shift the dose response. To adequately address this question, additional pharmacokinetic/pharmacodynamic studies are needed to determine target tissue dosimetry and dynamic response following chronic dietary exposure to CPF. Nonetheless, until additional data is available, the PBPK/PD model provides a reasonable qualitative assessment of the dose-dependent pharmacodynamic response that is observed in rats following chronic dietary administration of CPF.

Pharmacokinetics/pharmacodynamics of CPF in humans. The rodent PBPK/PD model was extended to incorporate human physiological constants, and the metabolic parameters were appropriately scaled as a function of body weight to enable the model to describe CPF dosimetry and dynamic response in humans. When available, parameters derived for human studies (*in vitro*/*in vivo*) were utilized in the model. Specifically, since human plasma ChE activity is primarily associated with a higher amount of BuChE vs. AChE (Ecobichon and Comeau, 1973) relative to the enzyme levels in rodent plasma, the amount of BuChE enzyme in the model of human plasma was increased (see Table 2) based on available data (Chan *et al.*, 1994). Nolan *et al.* (1984) conducted a controlled human study where volunteers were administered single doses of CPF orally (0.5 mg/kg) as well as dermally (5 mg/kg) and the pharmacokinetic and pharmacodynamic responses were then determined. This data set was utilized to calculate the appropriate elimination rate constant (Ke) and volume of distribution (Vd) to accurately describe the pharma-

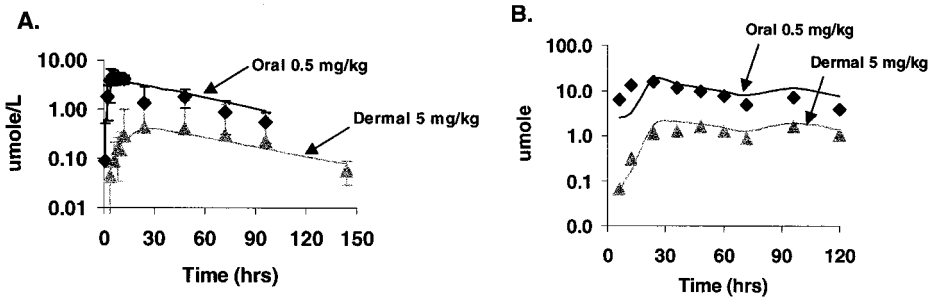

FIG. 6. Experimental data (symbols) from Nolan *et al*. (1984) and model simulations (lines) of the TCP pharmacokinetics in human volunteers administered an oral dose of 0.5 mg CPF/kg or a dermal dose of 5 mg CPF/kg. The time course data of TCP in the blood (A) represents the mean ± SD for 6 (oral) and 5 (dermal) male volunteers; (B) the amount of TCP excreted in the urine from the same volunteers.

cokinetics of TCP, and the dermal permeability coefficient (Kp) that was capable of accurately describing the extent and rate of dermal uptake of CPF. Secondly, the plasma BuChE enzyme activity and reactivation rate was optimized against the plasma BuChE inhibition data obtained following the single 0.5 mg CPF/kg oral dose. These model parameters were then held constant and model simulations were run against human pharmacokinetic data obtained within this study, and against limited pharmacokinetic data available in the literature (Drevenkar *et al.*, 1993).

Nolan *et al.* (1984) reported that the blood CPF concentrations following either oral or dermal exposure were extremely low (<0.085 nmol/ml) and exhibited no consistent temporal pattern; however the levels of the major metabolite TCP were readily quantifiable in both blood and urine following either dermal or oral administration. Therefore, the PBPK/PD model was used to characterize the TCP pharmacokinetics. Based on the amount of TCP excreted in the urine, it was determined that 70% ± 11 and 1.28% ± 0.83 of the oral and dermal dose of CPF was absorbed in these volunteers, respectively (Nolan *et al*., 1984). The time course of TCP in the blood and urine of these human volunteers, and the resulting model simulations following either a single oral 0.5-mg/kg or a dermal 5 mg/kg dose of CPF are presented in Figure 6. Following the oral or dermal dose, peak plasma TCP concentrations were 4.69 and 0.44 μmol/l and were attained at both 5 and 24 h postdosing. In addition, peak TCP urine excretion was achieved by 24 h postdosing for both the oral and dermal treatments, and the time course of urine excretion was very comparable for both dosing routes. Overall, the model provided a reasonable prediction of the route-dependent blood TCP kinetics following CPF exposure in humans.

Unlike the simple one-compartment model utilized to describe the fractional absorption of CPF in humans (Nolan *et al.*, 1984), the PBPK/PD model was modified to calculate the flux of CPF through the skin as a function of CPF permeability, concentration, area of exposed skin surface, and exposure length (Poet, 2000). Hence, the PBPK/PD model calculated a permeability coefficient (Kp) of 4.81×10^{-5} cm/h, and assumed a dermal exposure not exceeding 20 h postapplication; the estimated fractional absorption was 2.32%. This result is similar to the 1.28% and ~1% dermal absorption based on the recovery of TCP and dialkylphosphate metabolites in the urine, respectively (Nolan *et al*., 1984; Griffin *et al*., 1999). The time course of plasma BuChE inhibition kinetics following a single oral (0.5 mg/kg) or dermal (5 mg/kg) dose of CPF in human volunteers is presented in Figure 7. As previously noted, the amount of available plasma BuChE enzyme and the rate of enzyme recovery were optimized to fit the plasma BuChE inhibition time course following the oral 0.5 mg/kg CPF dose. The model parameters determined from the oral dosing study were then held constant and the PBPK/PD model was used to predict the extent of plasma BuChE inhibition following a 5 mg CPF/kg dermal exposure. Under this dermal exposure scenario, the model predicted maximum plasma BuChE inhibition of ~90% of control, which was comparable to the observed 87% seen with the experimental data; likewise the model reasonably predicted the enzyme recovery kinetics through 200 h postdosing.

Model predictions of effects of single, oral doses of CPF in human males and females. The model parameters for humans were derived from the literature and from fitting data from Nolan *et al*. (1984). Without altering the model parameters, the results of the controlled human CPF pharmacokinetic study, conducted as part of this project, were also compared against the PBPK/PD model predictions. There were no differences observed in the concentrations or time course of CPF and metabolites in these volunteers that was attributable to gender (data not shown). Following oral administration of CPF at doses ranging from 0.5 to 2 mg/kg, only 5 of the 12 volunteers

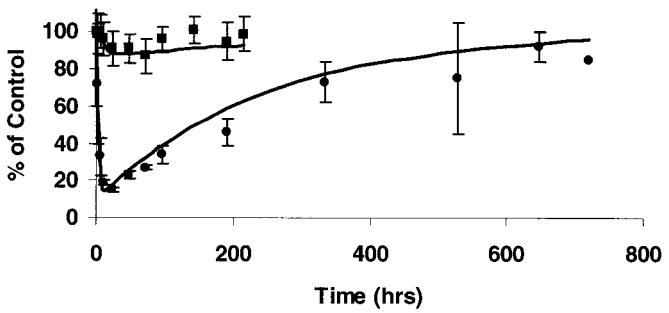

FIG. 7. Experimental data (symbols) from Nolan *et al*. (1984) and model simulations (lines) of the plasma ChE inhibition in human volunteers administered an oral dose (filled circles) of 0.5 mg CPF/kg or a dermal dose (filled squares) of 5 mg CPF/kg. The time course data represents the mean ± SD for 5 male volunteers.

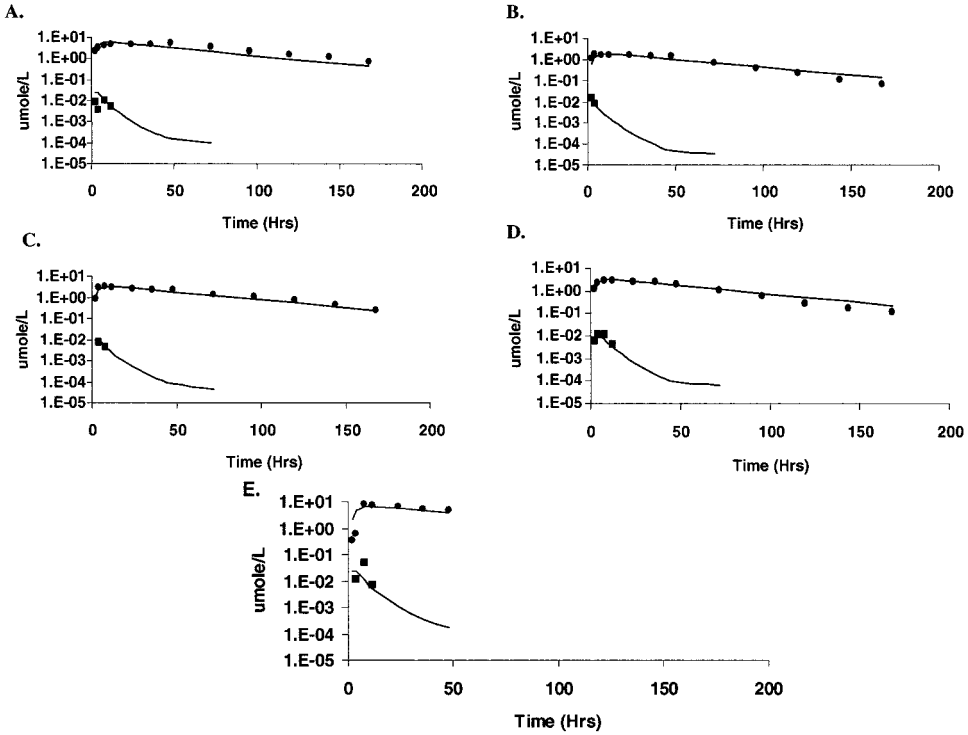

FIG. 8. Experimental data (symbols) and model simulations (lines) for the plasma concentration of TCP (filled circles) and CPF (filled squares) in 5 volunteers administered CPF as an oral dose of 1 mg/kg (A and B) or 2 mg/kg (C, D, and E). A–E, the individual results from the 5 volunteers.

on the study had quantifiable levels of CPF detected in a limited number of blood specimens and no CPF-oxon was detected in any specimens (LOQ = 3 nmol/l). The time course and model simulations of CPF and TCP concentrations in the blood of 5 volunteers (A–E) orally administered CPF at doses of 1 or 2 mg/kg are presented in Figure 8. Only one individual in this study, administered a dose of 2 mg CPF/kg, exhibited any RBC AChE inhibition (Volunteer E). The experimental data and model simulations indicate that CPF blood concentrations were at least 2 orders of magnitude less than the observed TCP blood concentrations, and all the blood specimens taken after 8 h postdosing were below quantitation limits for CPF. The model simulation was consistent with a rapid metabolic clearance of CPF, resulting in the formation of TCP, which had a considerably slower elimination rate and was readily detectable in the blood of these volunteers through 160 h post-dosing. Based on the model fit of these experimental data, the extent of oral absorption for these 5 volunteers ranged from ~18% to 38%, which is considerably less that the oral bioavailability of the 70% previously calculated for human volunteers, using a one-compartment model (Nolan *et al.*, 1984). The observed differences in oral bioavailability in these 2 studies are most likely associated with differences in dosage formulation (i.e., tablet vs. capsule).

Urine specimens were likewise analyzed for CPF, CPF-oxon, and TCP; however, neither CPF nor CPF-oxon was detected in any of the samples. The average TCP blood concentration and urine excretion time course for all human volunteers (male and female) administered 0.5, 1, or 2 mg CPF/kg as single oral doses are presented in Figure 9. Over the dose range evaluated, the kinetics of TCP in blood and urine were linear and proportional to dose. However, the model-predicted average oral fractional absorption for all treatment groups was ~20% of the orally administered dose, which was very close to the $AUC_{0-\alpha}$ estimation of 22.4% absorption of administered dose made from the TCP measurements in urine.

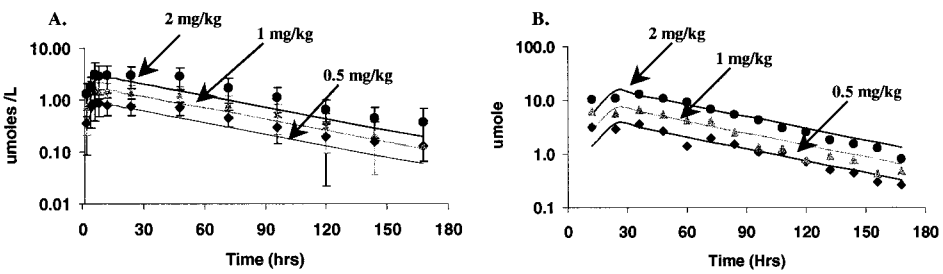

FIG. 9. Experimental data (symbols) and model simulations (lines) of the TCP pharmacokinetics in human volunteers administered oral doses of 0.5 (filled diamonds), 1 (filled triangles), and 2 (filled circles) mg CPF/kg. The time course data of TCP in the blood (A) represents the mean ± SD for 12 male/female volunteers; (B) the amount of TCP excreted in the urine is from the same volunteers.

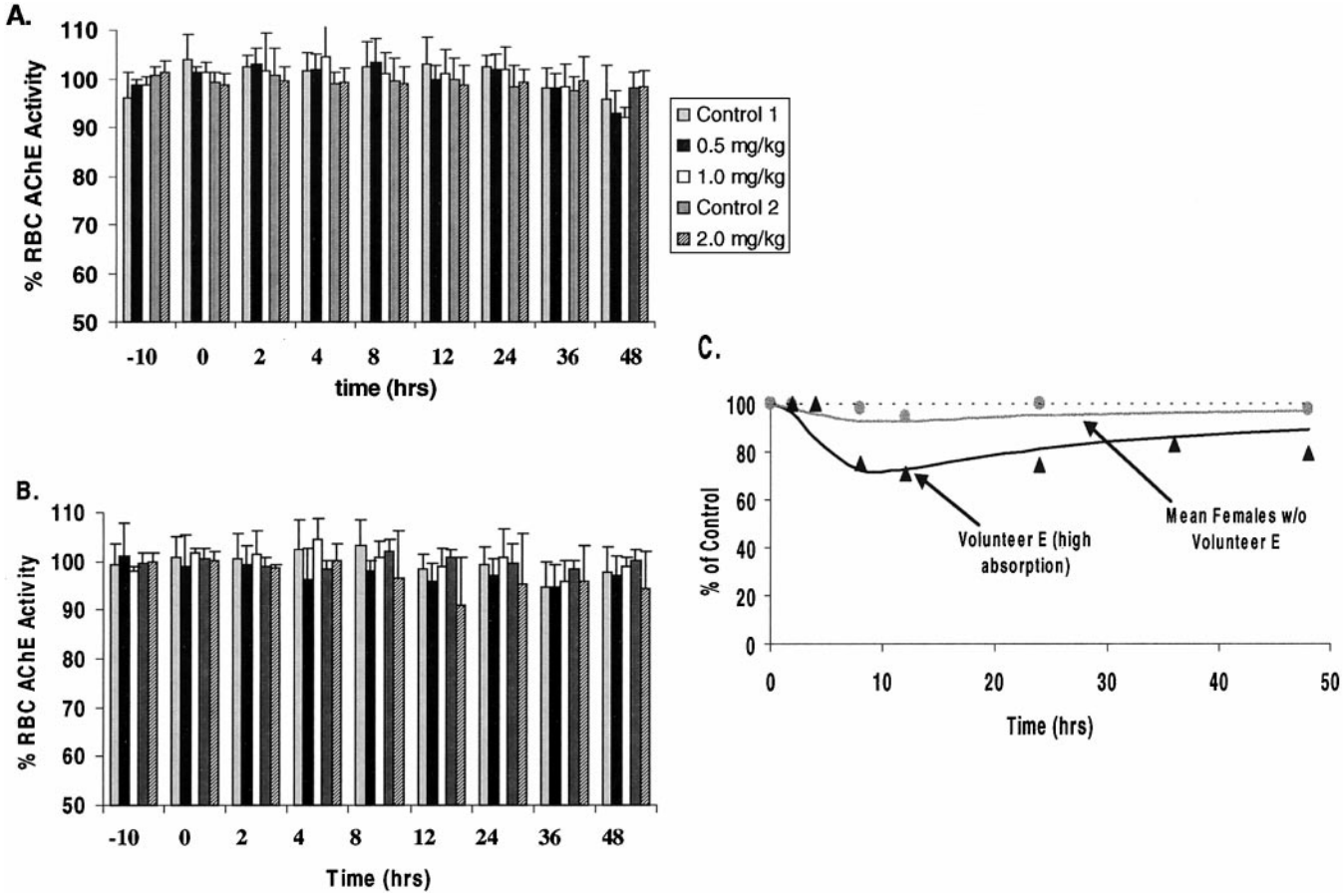

FIG. 10. RBC AChE activity in male (A) and female (B) volunteers presented as the mean ± SD for 6 volunteers administered CPF doses of 0 (Control), 0.5, 1, or 2 mg/kg of body weight, and the average control normalized RBC AChE activity (C) for the female 2-mg/kg treatments, with and without the inclusion of a single individual who was a high absorber. The symbols represent the observed data, while the line represents the model simulation. (Note: This study was conducted in two parts. Part 1 included control 1, 0.5, and 1 mg/kg doses; Part 2 included control 2 and 2 mg/kg dose).

The impact of single oral CPF doses (0.5, 1, or 2 mg/kg) on RBC AChE activity was assessed in these same human volunteers, and the results are presented in Figure 10. There was no inhibition of RBC AChE in males at any dose level (Fig. 10A). There was a slight decrease in RBC AChE activity in females, beginning at 8 h postdosing at the 2 mg/kg dose level (Fig. 10B). The decrease in RBC AChE activity appeared to be due to inhibition in one volunteer (Fig. 10C, Volunteer E). When data from the single volunteer was removed from the data set, the average RBC AChE activity in the remaining women ($n = 5$) was virtually indistinguishable from baseline.

Although the oral dose of CPF was 2 mg/kg body weight, the amount absorbed was appreciably less. For the 6 men and 5 women that had no RBC AChE inhibition, the urinary TCP $AUC_{0-\alpha}$, when corrected for average body weight, was comparable across gender at 2.97 and 2.78 mg/h/kg, respectively. Given an absorbed fraction of 0.70 of CPF that is recovered in urine as TCP (Nolan *et al*., 1984), the estimated average absorbed dose of CPF was 0.57 mg/kg. The woman with inhibited RBC AChE had about 2 times more TCP recovered from the urine (TCP $AUC_{0-\alpha}$, 5.55 mg/h/kg), which represented an estimated absorbed dose of 1.1 mg/kg of CPF. The model made a reasonable prediction of both the timing and degree of human RBC AChE activity for the woman with high absorption of CPF, and predicted little or no inhibition of the other 5 women that had less absorption (Fig. 10C).

Although only limited CPF blood time course data was available from the controlled human exposure (see Fig. 8) the model was capable of accurately describing the CPF blood kinetics. To further validate the capability of the model to accurately describe the pharmacokinetics of CPF, the time course of CPF in serum from an individual who ingested a concentrated formulation of CPF (Drevenkar *et al*., 1993) was modeled and the results are presented in Figure 11. The subject was a 25-year-old male reported to have drunk 30–60 ml of a commercially available insecticide that contained CPF as the active ingredient. The subject was admitted to the hospital 2 to 5 h after ingestion of the pesticide formulation, and CPF was quantitated in the serum for up to 15 days after poisoning. The samples were likewise analyzed for CPF-oxon; however the

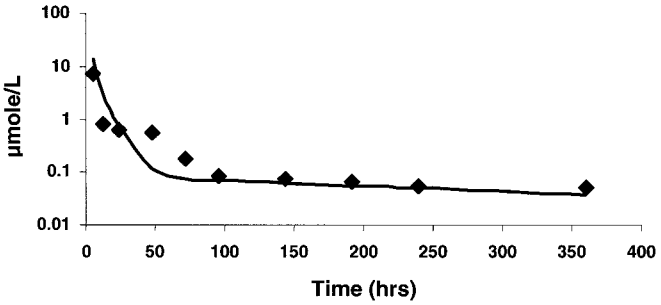

FIG. 11. Time course of CPF in serum of a single poison victim that orally ingested a commercial insecticide product containing CPF (data extracted from Drevenkar *et al*., 1993). The symbols represent the observed data while the line represents the model simulation.

oxon was not detectable in any of the samples (Drevenkar *et al*., 1993). The PBPK/PD model was capable of accurately describing the overall pharmacokinetics of CPF in the blood following a single acute exposure. Based on the observed CPF blood time course, the model estimated that an acutely toxic dose of ~180 mg/kg was needed to achieve the highest concentrations of CPF (1–10 μmol/l) that were detected in the serum. This predicted dosage is well within the range of reported acute LD_{50} doses (85–504 mg/kg) in animals, and is a reasonably good approximation of a dosage that is capable of producing the reported acute toxicological responses in humans (Gaines 1969; McCollister *et al*., 1974).

DISCUSSION

Thionophosphorus organophosphates such as CPF constitute a large class of chemical insecticides that have seen widespread utilization in both agriculture and home applications. The potential for OP insecticides to produce a toxic response is dependent upon the balance between the amount of delivered dose to the target site and the rates of bioactivation and/or detoxification (Calabrese, 1991). In order to quantitatively integrate all the physiological, metabolic, and biochemical factors associated with CPF absorption, distribution, metabolism to CPF-oxon and TCP, and the resulting ChE inhibition, a PBPK/PD model was developed for both rats and humans. Overall, the results presented here illustrate that the current model can reasonably describe rat and human dosimetry and dynamic response data under a broad range of exposure scenarios (acute vs. chronic, oral vs. dermal). However, it is also recognized that some model fits could be improved upon, which supports the need for additional experimental data, including better parameter estimates, to facilitate future model refinement.

In developing the CPF model it became obvious that, although a considerable amount of hazard evaluation research has been performed on CPF, only a limited number of pharmacokinetic studies were available for model development. Therefore, both rat and human pharmacokinetic/pharmacodynamic studies were conducted to provide the needed experimental data to develop and validate the model. Utilizing recently developed sensitive (i.e., low ppb range) analytical methods (Brzak *et al*., 1998) it was feasible to quantitate CPF, CPF-oxon, and TCP following *in vivo* exposures to CPF and to directly link dosimetry with the observed ChE and AChE inhibition kinetics in both rats and humans.

The PBPK/PD model provides important insights into the route- and dose formulation-dependent absorption of CPF in rats and humans. Due to its poor aqueous solubility, CPF dose solutions are generally prepared in an oil-based matrix (e.g., corn oil) and administered to rodents by oral gavage. Previous studies have shown that the dosing vehicle can modify the amount and rate of absorption, and corn oil in particular has been shown to result in lower peak and increased time to maximum blood concentrations (C_{max}) (Withey *et al.*, 1983). Hence, to describe the uptake of CPF from the GI tract of rats, we needed a two-compartment GI tract model similar to the one used to describe the uptake of chlorinated solvents (Staats *et al*., 1991). This model modification resulted in a more accurate simulation of CPF uptake than was feasible with the single-compartment model, although it did not enable the model to adequately fit the peak blood (3 h postdosing) CPF concentration. In addition to a slower overall rate of uptake, due to corn oil, the amount of CPF orally absorbed in rats was estimated to be ~80%. This estimate was based on pharmacokinetic studies where rats were administered ^{14}C-labeled CPF and the ^{14}C activity was determined in tissues and excreta (Dow Chemical, unpublished report). Differences in the extent of CPF absorption were also clearly evident when comparing the human CPF pharmacokinetics conducted in this study with the results from human kinetic studies conducted under different dosing conditions. Nolan *et al.* (1984) deposited a known amount of CPF onto a lactose tablet, which was subsequently swallowed with water. This dose preparation resulted in ~70% of the orally administered dose being recovered as TCP. In contrast, the CPF dose in the current human kinetic study was prepared by adding CPF and lactose as dry powders into a dissolvable capsule that was likewise swallowed with water, however only 20–35% of this oral dose was recovered as TCP. Based on these experimental findings, the extent of CPF absorption appears to be dependent upon its physical form when administered. The question of bioavailability is of particular importance when interpreting a ChE response based only upon the administered dose, without taking into full consideration how much of that dose was actually absorbed. Therefore, interpretation of pharmacodynamic response data would certainly be strengthened with a concurrent assessment of bioavailability within the same study. This analysis could readily be accomplished by quantitating blood or urinary TCP concentrations. However, for the purposes of the rat PBPK/PD model development, the oral absorption of CPF, using a corn oil dosing matrix, was set at 80% for all model simulations. This assumption was made while fully recognizing that it represents

an oversimplification, since the extent of absorption can be drastically different depending on the conditions of the dose solution (i.e., formulation), dosing method, and variations in species, gender, or strain (Kararli, 1995).

In reality the majority of both occupational and environmental exposures to OPs are primarily associated with the dermal route, which has been reported to account for more than 90% of the systemically absorbed dose in humans (Aprea *et al*., 1994). Therefore, an understanding of percutaneous absorption of OPs is critical for quantitatively determining a systemic dose. The extent of *in vivo* dermal absorption of CPF in humans has previously been reported as low (1–3%; Griffin *et al.*, 1999; Nolan *et al*., 1984). This is consistent with the low *in vivo* dermal absorption potential reported in humans exposed to diazinon, isofenphos, and malathion, which ranged from 2.5–3.9% of the applied dose (Wester *et al*., 1983; 1992; 1993). In the current PBPK/PD model, the dermal uptake of CPF in humans was well described by estimating a CPF permeability coefficient (Kp) of 4.81×10^{-5}/cm/h utilizing previously published dermal absorption data in humans (Nolan *et al*., 1984). The model presented herein quantitatively predicts the concentration of CPF, CPF-oxon, and TCP in blood, tissues, and excreta in both rats, and humans following exposure, either orally or through direct skin contact, with CPF. These results are consistent with TCP being the major metabolite formed that attained a blood concentration of 100-fold higher than the parent compound (see Fig. 8). Likewise, the pharmacokinetic studies conducted in rats suggest that levels of CPF in the blood exceed the CPF-oxon concentrations. These results clearly indicate that even when employing sensitive analytical techniques, quantifiable concentrations of both CPF and CPF-oxon in blood are only obtainable when relatively high doses of CPF (>5 mg/kg) were administered, and even then, it was only detectable for a limited time after dosing. This inability to adequately quantitate both CPF and CPF-oxon blood concentrations over a range of dose levels has made it particularly challenging to accurately model dosimetry, particularly at low doses (<10 mg/kg).

Biomonitoring of OPs and their metabolites in blood and urine has been used to provide a quantitative assessment of dosimetry in human poison victims following acute high-dose exposure (Drevenkar *et al.*, 1993; Vasilic *et al.*, 1992), and for the assessment of secondary exposures (Loewenherz *et al*., 1997; Richter *et al.*, 1992). A major advantage in utilizing the analysis of intact pesticide or specific metabolites in body fluids versus ChE depressions is that it enables identification of specific chemical agent(s) that may be associated with the observed esterase inhibition (Ellenhorn and Barceloux, 1988; Lotti *et al.*, 1986), and as previously mentioned, can be used to better determine bioavailabilty. The utilization of PBPK/PD models such as the one developed for CPF enables the quantitative integration of dosimetry with biological response. The model can predict the extent of esterase inhibition (see Fig. 7) based on the observed concentrations of either the parent compound (see Figs. 8 and 11) or metabolites (see Figs. 6, 8, 9). Hence this PBPK/PD model provides an integrated assessment of CPF dosimetry and biological response in both rats and humans for a number of exposure scenarios.

The PBPK/PD model integrates CPF dosimetry with a pharmacodynamic model capable of predicting stoichiometric B-EST inhibition, and is consistent with other pharmacodynamic models such as the one developed for soman in the rat (Maxwell *et al*., 1988). The extent and rate of B-EST inhibition and recovery is dependent upon the amount of available enzyme, the Ki, and the amount of time the B-EST is exposed to the available oxon (Vale, 1998). As previously noted, the amount of available B-EST binding sites (μmol) in general followed the order CaE >> BuChE $\approx$ AChE (Maxwell *et al*., 1987), whereas the Ki rates followed the order: BuChE >> AChE > CaE. Initial model simulations utilized relatively higher Ki values determined with purified BuChE and AChE enzyme (Amitai *et al*., 1998), which severely over predicted the extent of ChE and AChE inhibition (data not shown). In this regard, Mortensen *et al.* (1998) noted differences in *in vitro* sensitivity (i.e., IC_{50s}) of AChE when comparing the inhibition of purified enzyme against crude tissue homogenates. Hence it is not unreasonable to expect that the Ki values determined with purified enzymes would not adequately describe the inhibition response obtained with crude enzyme preparations. Therefore, an apparent Ki was determined for CPF-oxon inhibition of B-EST enzymes that was qualitatively consistent with the Ki values measured with purified enzymes (Amitai *et al.*, 1998). The model simulation suggests that BuChE is the most sensitive to CPF-oxon inhibition due to a higher apparent Ki (2.0×10^3 μM/h) and relatively low amounts ($\sim$1600 μmol total in rat) of available BuChE in the tissues. In contrast, the model predicts that CaE is the least sensitive to CPF-oxon, and appears to be due to the combination of an estimated low apparent Ki (20 μM/h), and high amounts of available enzyme (2×10^6 μmol total in rat). Finally, the sensitivity of AChE enzyme to CPF-oxon inhibition resulted from a moderate (between BuChE and CaE) apparent Ki (243 μM/h), and relatively low amounts ($\sim$1000 μmol total in rat) of available AChE enzyme. Although these apparent Ki parameter estimates provide a reasonable description of the B-EST inhibition kinetics, it is clear that the model would be further strengthened by experimentally determining these Ki parameters under physiological conditions that more accurately reflect *in vivo* activity. In addition, uncertainty associated with model estimates of CPF-oxon concentration raises the possibility that the model overestimates of CPF-oxon concentration, particularly at high doses, may have contributed to excessive esterase inhibition predictions. Additional quantitative data on CPF-oxon blood and/or tissue concentrations and Ki parameter estimates may help resolve this question.

Chanda *et al.* (1997) evaluated the tissue-specific effects of CPF on both CaE and ChE, utilizing *in vivo* and *in vitro* comparisons. They reported that the maximum inhibition of

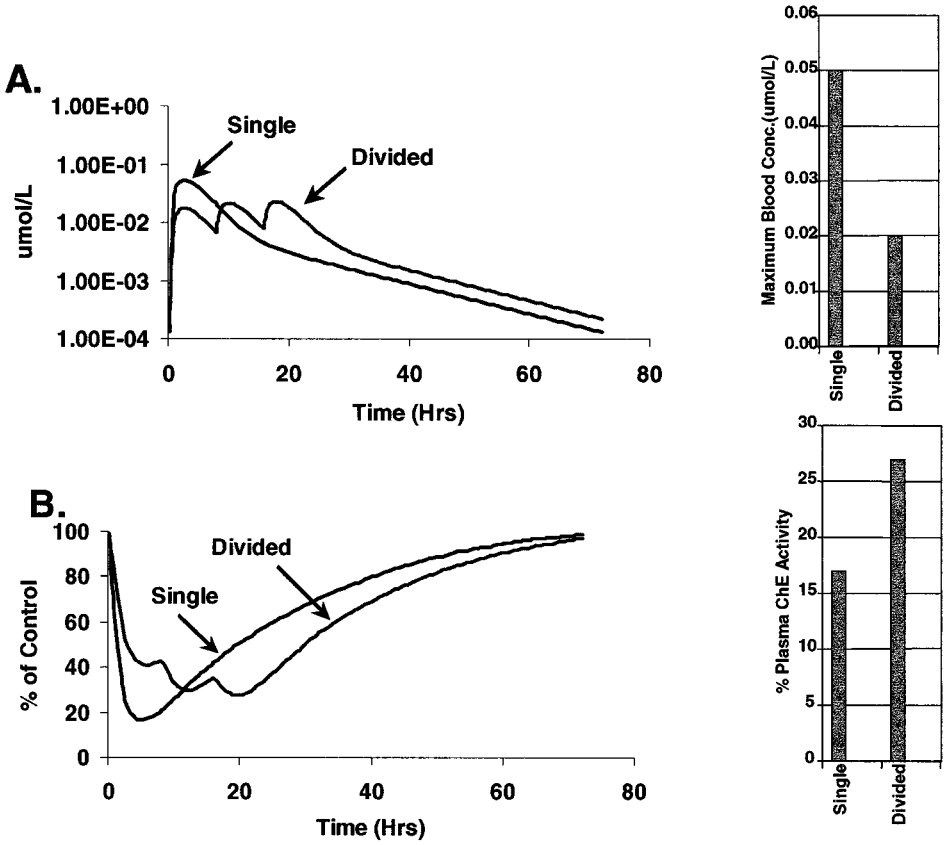

FIG. 12. Simulated concentration of CPF in blood (A) and ChE inhibition in plasma (B) following oral administration of a single dose of CPF (10 mg/kg), or the same dose divided (3 × 3.3 mg/kg, at 8-h intervals) over the first 24-h interval.

plasma CaE, following an 80-mg CPF/kg dose, was ~40% of control (Chanda *et al.*, 1997), whereas, in the current study, a comparable level of plasma ChE (50:50—BuChE: AChE) inhibition was achieved at a dose level of ~5 mg CPF/kg (see Fig, 2). These results are consistent with the observed differences in apparent Ki's, and the amounts of available B-EST enzymes in the rat. Likewise, these results are consistent with the observation that B-EST inhibition is an integrated function of target-tissue dosimetry, esterase affinity for CPF-oxon, and the number of available esterase binding sites in each tissue compartment. In this regard, improvements in the predictive capability of the current model may be achieved by conducting studies that better characterize the time course of specific esterase activities (i.e., AChE, BuChE, and CaE) in both blood and tissue compartments over a broad range of CPF exposures.

It has been generally accepted that the biological bases of risk assessments are strengthened by the utilization of an internal dose surrogate versus the administered dose in cross-species extrapolations (Andersen, 1995). A determination of dose-rate effect may also be important, since under the Food Quality Protection Act (FQPA) there is concern about the risk associated with pesticide residue exposures where dermal contact and/or ingestion of low levels of pesticide residue on food constitute important exposure routes (U.S. EPA, 1998). In this case, an evaluation of maximum blood concentration (C_{max}) and/or blood AUC is of relevance since these dose surrogates may be particularly sensitive to dosing rate (Corley, *et al.*, 1994). To illustrate this point, a simulation of the blood CPF concentration and plasma ChE response in rats following either a single bolus dose of 10 mg CPF/kg or the same dose fractionated (3 × 3.3 mg/kg at 8-h intervals) over a 24-h period is presented in Figure 12. Based on model simulations, the C_{max} for blood CPF was ~ 0.05 μmol/l, whereas the same dose when fractionated over a 24-h period attained a C_{max} of ~0.02 μmol/l. Although the blood concentration for the fractionated dose was slightly less than half of that obtained following the bolus administration, repetitive dosing did result in the blood levels of CPF being maintained at elevated levels until dosing ceased (~24 h). The potential impact of dividing the dose was particularly evident when comparing the model simulation of ChE inhibition (see Fig. 12 B). Compared to bolus administration, dividing the dose reduced the peak inhibition by ~10% (~27% of control). These simulations infer that the administration of CPF as a large bolus dose, results in a greater maximum plasma ChE inhibition than when the same dose is administered over a prolonged time period (i.e., divided). Based on these model simulations, future studies should consider experimentally determining the impact of dose-rate on both CPF dosimetry and dynamic response.

Simulations of the $AUC_{0-\alpha}$ for the concentration of CPF in blood and CPF-oxon in both blood and brain for rats and humans acutely exposed by oral ingestion to a broad range of

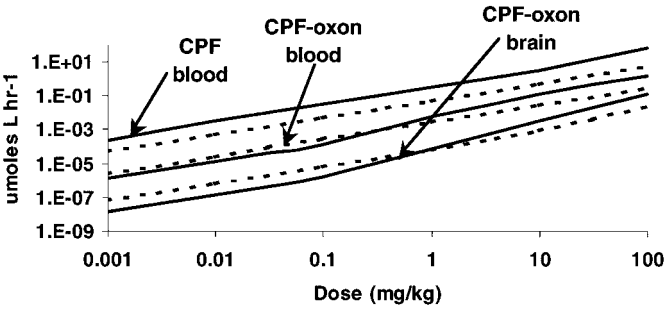

FIG. 13. Simulation of the area under the concentration curve ($AUC_{0-\alpha}$) for CPF in blood and CPF-oxon in blood and brain in rats (dashed lines) and humans (solid lines) following an acute exposure to a broad range of CPF doses.

CPF doses (0.001–100 mg/kg) is presented in Figure 13. To compare the response at equivalent doses between species, the oral absorption was set at 80%. In both rats and humans, the $AUC_{0-\alpha}$ followed the order: CPF (blood) > CPF-oxon (blood) > CPF-oxon (brain). Over the dose range evaluated, the CPF blood $AUC_{0-\alpha}$ ranged from ~4–13-fold higher in humans than in rats and demonstrated a slightly increasing trend with dose. In contrast, at low doses (<1 mg/kg), the $AUC_{0-\alpha}$ for CPF-oxon (blood and brain) in rats was ~2–4-fold higher than at comparable doses in humans. However, in humans, increasing the dose above 1 mg/kg resulted in a nonlinear "crossover" response so that at high doses the simulated human $AUC_{0-\alpha}$ for CPF-oxon (blood and brain) exceeded that of the rat (~1.1–6-fold). Although these simulation results must be evaluated, taking into full consideration the uncertainty in the model predictions of the CPF and CPF-oxon concentrations, the simulation is consistent with a response where one or more of the detoxification pathways has become overwhelmed.

As previously noted, the extent of CYP450 activation of CPF to CPF-oxon and differences in detoxification are most likely responsible for any observed species-dependent increased sensitivity. Since tissue and blood B-EST stoichiometrically bind to oxon and become irreversibly inactivated (Chandra *et al.*, 1997; Clement, 1984), one reasonable hypothesis is that the dose-dependent depletion of nontarget B-EST is a key component contributing to the observed species differences in the dose response for AChE inhibition. Therefore, by comparing the dose-dependent inhibition of plasma ChE in rats and humans, it may be possible to illustrate the potential protective role of nontarget B-EST. However, it is important to recognize that across species there are marked quantitative differences in the amount of available B-EST (Ecobichon and Comeau, 1973). For example, as previously noted in rat plasma, ChE is the sum of both plasma AChE and BuChE activity (Maxwell *et al.*, 1987), whereas in humans, plasma ChE is exclusively BuChE (ONRL, 2000). A simulation of the maximum plasma ChE response in rats and humans, following acute oral exposure to a broad range of CPF doses (0.001 to 100 mg/kg), is presented in Figure 14. To compare the responses between rats and humans, at equivalent systemic doses, the oral absorption was set at 80%. In the model simulation, both rat and human plasma BuChE have a similar dose response and are essentially depleted at doses between 1 and 10 mg/kg. However in the rat, the available plasma AChE enzyme is not depleted until the dosage is ≥10 mg/kg. These results are consistent with the dose-dependent $AUC_{0-\alpha}$ simulations for CPF and CPF-oxon (see Fig. 13) and suggest a plausible relationship between the extent of CPF activation, the depletion of nontarget B-EST, and the nonlinear increase in human CPF-oxon blood and brain concentration at doses ≥1 mg/kg. It is important to realize that in assessing plasma esterase activity, a single substrate, acetylthiocholine (AcTh), is routinely utilized for plasma ChE determinations, although AcTh has a greater specificity for AChE than for BuChE enzyme (Venkataraman and Rani, 1994; ORNL, 2000). This analytical approach has made it particularly challenging to model the rodent esterase response in compartments, like blood, where both AChE and BuChE enzymes are available to CPF-oxon for binding and inhibition. Therefore, in accessing the protective role of nontarget B-EST it is important to carefully consider the contribution of multiple esterases and the importance of enzyme substrate specificity in determining enzyme inhibition.

Rat and human data on inhibition of RBC AChE are also consistent with the PBPK model. The model estimates similar levels of CPF oxon in the blood of humans and rats, particularly at doses around 0.2 to 0.5 mg/kg (Fig. 13). Based upon absorbed doses of CPF, humans and rats also had similar profiles of inhibition of RBC AChE. There was no inhibition of RBC AChE in humans that had an absorbed dose of 0.57 mg/kg, and an absorbed dose of 1.1 mg/kg caused approximately 25% inhibition in one human volunteer (Fig. 10C). Rats given an oral gavage dose of 0.75 mg/kg had no inhibition of RBC AChE, and an oral dose of 1.5 mg/kg caused about 30% inhibition (4 h postdose, Zheng *et al.*, 2000). Thus, based upon modeled estimates of blood CPF oxon and RBC AChE inhibition, there appeared to be little difference between rat and human RBC AChE responses at this dose range.

Although the current PBPK/PD model describes the phar-

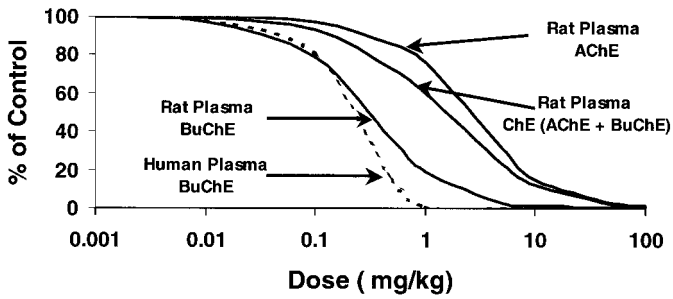

FIG. 14. Simulation of peak plasma total ChE (AChE + BuChE), AChE and BuChE inhibition dose response in rats and humans BuChE following an acute exposure to a broad range of CPF doses.

macokinetics and pharmacodynamics of CPF over a broad dose range (0.5–100 mg/kg), it is important to recognize that even the lowest doses evaluated in the current study are still significantly greater than typical aggregate (total dietary and residential) human exposures. In both adults and children, potential aggregate exposures to CPF are estimated to range from 0.46 to 1.7 μg/kg/day, which is ~294- to 1000-fold below the lowest dose (0.5 mg/kg) used in this study (Gibson *et al.*, 1999; Hill *et al*., 1995; Quackenboss *et al*., 1998; Shurdut *et al*., 1998;). Based upon the observed dose response, where CPF and CPF-oxon were nondetectable and blood ChE activity was minimally depressed at doses of 0.5 mg/kg, it is hypothesized that a significant first-pass metabolism will be observed at environmentally relevant doses. In this regard, a number of recent studies have demonstrated that intestinal epithelial cells have CYP450 metabolic capacity and are capable of significantly altering oral bioavailability of drugs and chemicals in animals and humans (Hall *et al.*, 1999; Obach *et al.*, 2001; Paine *et al.*, 1999; Schmiedlin-Ren *et al.*, 1993; Watkins, 1992; Zhang *et al.*, 1999). A number of the CYP450 isoforms residing within the intestines have been shown to metabolize a number of OP insecticides including parathion, diazinon, and CPF (Butler and Murray, 1997; Fabrizi *et al*., 1999; Sams *et al*., 2000). In addition, P-glycoproteins (multidrug resistance proteins) are located in the apical borders of intestinal cells, and are known to be upregulated and bound by CPF-oxon (Lanning *et al.*, 1996). Thus, an unknown amount of first-pass CPF detoxification and activation should occur in the intestines, and CPF-oxon that is generated in enterocytes would be subject to removal by P-glycoproteins. Since the current model does not incorporate intestinal metabolism or P-glycoprotein removal of CPF-oxon, it is anticipated that the model overestimates low-dose oral bioavailability, thereby potentially overpredicting dosimetry and dynamic response. Therefore, to address this important question, research is ongoing to further refine the PBPK/PD model with the inclusion of a metabolically active intestinal compartment, and associated studies are being conducted to validate the model response at environmentally relevant exposures.

The PBPK/PD model that was developed for CPF is capable of quantitating target tissue dosimetry and dynamic response in both rats and humans, and is a useful tool to quantitatively assess risk associated with CPF exposure as well as helping to design and focus future experimental research. The capability of the model to accurately predict dosimetry and response is limited by the adequacy of the model parameters and limitations of the experimental data. As with all models, developing and validating a PBPK/PD model is an iterative process and highlights the current limitations of our understanding of critical biological processes that help identify important data gaps. Additional research could provide a better characterization of the absorption kinetics and dosimetry for CPF and CPF-oxon under various dosing conditions. Of particular importance are experimental data to better understand the extent of CPF absorption at environmentally relevant exposures, and to evaluate the potential role of gut metabolism and CPF-oxon protein binding following low-dose exposures. Additional studies could better characterize the time course and dose response for RBC AChE inhibition, since this pharmacodynamic response is particularly relevant as a potential biomarker for exposure. Better parameter estimates are needed for the binding of CPF-oxon with B-EST and in particular the CaE tissue inhibition kinetic parameters for both rats and humans. In conclusion, this CPF PBPK/PD model quantitatively estimates target tissue dosimetry and AChE inhibition, and is an effective framework for future OP model development, and for establishing a biologically based risk assessment for CPF exposure under a variety of scenarios.

APPENDIX

Differential equations and abbreviations for the various tissue compartments utilized in the PBPK/PD model different from those of Gearhart *et al.* (1990) are listed below:

Oral absorption (gavage). The absorption of CPF following oral administration in corn oil vehicle was modeled utilizing a two-compartment model. The rate of change and amount of CPF in the compartments is described as

$$\frac{dCmpt1}{dt} = -\mathrm{KaS} * \mathrm{Cmpt1} - \mathrm{KsI} * \mathrm{Cmpt1}$$

$$Cmpt1 = \int_0^t d\mathrm{Cmpt1}dt.$$

$$\frac{dCmpt2}{dt} = \mathrm{KsI} * \mathrm{Cmpt1} - \mathrm{KaI} * \mathrm{Cmpt2}$$

$$Cmpt2 = \int_0^t d\mathrm{Cmpt2}dt,$$

$$\frac{dOral}{dt} = \mathrm{KaS} * \mathrm{Cmpt1} + \mathrm{KaI} * \mathrm{Cmpt2}$$

where KaS and KaI are the 1st-order rate constant (hr^{-1}) for absorption from the 1st and 2nd compartments (Cmpts 1 and 2) into the liver compartment, and KsI (h^{-1}) is the transfer rate constant between GI tract compartments. The rate of oral absorption (*d*Oraldt) is the sum of the absorption rates from Cmpt1 and Cmpt2.

Oral absorption (dietary). To model dietary administration of CPF, the dietary update was modeled as a zero-order process, and was based on the equations used to describe uptake from drinking water (Andersen *et al*., 1987 and Corley *et al*., 1994) as

$$\mathrm{k_{zero}} = \frac{\mathrm{Diet} * \mathrm{Fa}}{12\ \mathrm{hr}},$$

where Diet is the dietary dose of CPF (μg/kg/day), and Fa is the fractional absorption (%) of CPF from the diet. The k_{zero} was the zero-order uptake rate (μmol/h) of CPF from the diet. To model repeated dosing, a 24-h pulsing routine was incorporated into the model in which food containing CPF was consumed for a 12-h period over each 24-h interval. The amount of CPF absorbed from either the gavage or dietary administration was added directly into the liver compartment.

Dermal absorption. The rate of change in the amount of CPF absorbed through the skin (ASK, μmol) was described based on previous dermal uptake PBPK models (Corley *et al.,* 1994; McDougal *et al.,* 1986) as

$$\frac{dADL}{dt} = \frac{\text{Kp} * \text{SA}}{1000} * \left(\text{ConcL} - \frac{\text{ADL}}{\text{Vliq}}\right),$$

$$ADL = \int_0^t d\text{ADL}dt,$$

$$\frac{dASK}{dt} = \text{QSK} * (\text{Caf} - \text{CVskf}) + \frac{dADL}{dt},$$

$$ASK = \int_0^t d\text{ASK}dt,$$

where, *d*ADLdt is the rate of change of CPF in the skin, Kp is the permeability constant for CPF (cm/h), SA is the surface area exposed (cm^2), ConcL is the concentration of CPF in liquid (μmol/l), ADL is the amount of CPF in the skin (μmol), and Vliq is the initial volume of liquid applied to skin (L), QSK is the blood flow to the skin (L/h), CAf is the free concentration of CPF in arterial blood (μmol/l), and CVskf is the concentration of free CPF in venous blood draining the skin (μmol/l).

Liver compartment. The rate of change in the amount of CPF in the liver (AH, μmol) is described as the rate of free CPF entering the liver as absorbed dose from the GI tract, or through the systemic circulation minus the rate of free CPF leaving the liver unchanged, or by metabolism to either CPF-oxon or TCP as

$$\frac{dAH}{dt} = \text{QH} * (\text{CAHf} - \text{CVHf}) + \frac{dOral}{dt} - \frac{dAML1}{dt} - \frac{dAML2}{dt}$$

$$\frac{dAML1}{dt} = \frac{\text{Vmax1} * \text{CH}}{\text{Km1} + \text{CH}}$$

$$\frac{dAML2}{dt} = \frac{\text{Vmax2} * \text{CH}}{\text{Km2} + \text{CH}}$$

$$AH = \int_0^t d\text{AH}dt$$

$$\text{CH} = \frac{\text{AH}}{\text{VH}}$$

where QH is the blood flow (l/h) to the liver, CAHf and CVHf are the concentrations (μmol/l) of free CPF in arterial blood entering the liver and CPF in venous blood draining the liver, respectively. *d*Oraldt is the rate of uptake (μmol/h) into the liver compartment from the GI tract, AML1 and AML2 are the amounts (μmol) of free CPF metabolized to CPF-oxon and TCP by hepatic CYP450, respectively. V_{max1} and K_{m1} are the maximum velocity (μmol/h) and the Michaelis constant (μmol/l) for metabolism to CPF-oxon, respectively, and V_{max2} and K_{m2} are the maximum velocity (μmol/h) and the Michaelis constant (μmol/l) for metabolism to TCP, respectively.

Protein binding of CPF and CPF-oxon. The protein binding of CPF (FBc) and CPF-oxon (Fbo) were set at a constant fraction (%). Only free (i.e., nonbound fraction) CPF, or CPF-oxon were allowed to partition into and out of each tissue compartment and be available for metabolism (i.e., CYP450, B-EST, A-EST). The concentration of bound CPF or CPF-oxon in both arterial and venous blood was continuously calculated as a function of the free CPF or CPF-oxon in arterial blood or in venous blood draining each tissue compartment to maintain mass balance; the protein binding in plasma was calculated by the equations

$$\text{CV} = \sum \frac{(\text{Qi} * \text{CVif})}{\text{QC}} + \frac{(\text{Qi} * \text{CVib})}{\text{QC}},$$

$$\frac{dABl}{dt} = \text{QC} * (\text{CV} - \text{CA}),$$

$$ABl = \int_0^t d\text{ABl}dt,$$

$$\text{CA} = \frac{\text{ABl}}{\text{VBl}},$$

$$\text{CAf} = \text{CA} * (1 - \text{FB}),$$

$$\text{CAb} = \text{CA} * \text{FB},$$

where CV is the pooled venous blood which is the sum of the free and bound CPF or CPF-oxon concentrations (μmol/l) in the venous blood draining all the compartments, Qi is the blood flow to each tissue compartment (l/h), Cv*i*f and Cv*i*b are the concentrations of free and bound CPF or CPF-oxon, respectively, in the venous blood draining each compartment, and QC is the cardiac output (l/h). The total amount of CPF or CPF-oxon and their concentrations in the blood compartment are ABl (μmol), and CA (μmol/l), and CAf, and CAb are the concentration of free and bound CPF or CPF-oxon, respectively, in the arterial blood.

Liver compartment CPF-oxon model. The liver compartment represents the linkage between the models for CPF and CPF-oxon (See Fig. 1). The rate of change in the amount of CPF-oxon in the liver (AHo, μmol) is defined as the rate of input from the metabolism of CPF to CPF-oxon (*d*AML1dt), plus the input from the hepatic artery, minus the rate of loss into the venous blood draining the liver (CVHof), where the blood concentrations available for partitioning of CPF-oxon into and out of the liver are not bound to protein (i.e., free). Additional loss of free CPF-oxon is associated with hepatic A-EST and B-EST metabolism. according to the equations

$$\frac{dAHo}{dt} = \text{QH} * (\text{CAHof} - \text{CVHof}) + \frac{dAML1}{dt} - \frac{dAML3}{dt} - \left(\frac{dAML4}{dt} + \frac{dAML5}{dt} + \frac{dAML6}{dt}\right),$$

$$\frac{dAML3}{dt} = \frac{\text{Vmax3} * \text{CHo}}{\text{Km3} + \text{CHo}},$$

$$\frac{dAML(4-6)}{dt} = \text{AHce} * \text{Ki} * \text{CHo},$$

$$AHo = \int_0^t d\text{AHo}dt,$$

$$\text{CHo} = \frac{\text{AHo}}{\text{VH}},$$

where the rate of A-EST metabolism (*d*AML3dt) of CPF-oxon to TCP is described by Michaelis-Menten kinetics, $Vmax_3$, and Km_3 are the maximum velocity (μmol/h) and Michaelis constant (μmol/l), and the rate (μmol/h) of hepatic B-EST (i.e., AChE, BuChE, and CaE) metabolism of CPF-oxon to TCP calculated as the product of the amount of available enzymes (AHce, μmol), bimolecular inhibition rate constant (Ki, μM/h), and the concentration of CPF-oxon (CHo, μmol/l) in the liver compartment. Similar equations for B-EST metabolism of CPF-oxon to TCP were included in the blood, diaphragm, and brain compartments; in addition, A-EST metabolism of CPF-oxon to CPF was also incorporated into the blood compartment.

Tissue concentrations of CPF or CPF-oxon. The rate of change of CPF or CPF-oxon in tissues that neither form nor eliminate CPF-oxon is similar to that of Corley *et al.* (1994), as

$$\frac{dAi}{dt} = \mathrm{Qi} * (\mathrm{CAif} - \mathrm{CVif}),$$

where *Ai* is the amount of CPF or CPF-oxon in the *i* tissue (μmol/l), and CA*i*f and CV*i*f are the free concentrations (μmol/l) in the arterial and venous blood entering and draining, respectively.

B-EST tissue inhibition by CPF-oxon. The equations describing the tissue (i.e., blood, brain, diaphragm, and liver) inhibition of AChE, BuChE, and CaE by CPF-oxon are similar to those used to describe B-EST inhibition by DFP (Gearhart, *et al*., 1990). For example, the equations describing ChE inhibition in the liver compartments are

$$\frac{dAHce}{dt} = \mathrm{Ks} - \mathrm{AHce} * (\mathrm{Kd} + \mathrm{Ki} * \mathrm{CHo}) + \mathrm{INactive} * \mathrm{Kr},$$

$$\mathrm{AHce} = \int_{Ince}^{t} d\mathrm{AHce}dt,$$

$$\frac{dINactive}{dt} = \mathrm{AHce} * \mathrm{Ki} * \mathrm{CHo} - \mathrm{INactive} * (\mathrm{Ka} + \mathrm{Kr}),$$

$$INactive = \int_{0}^{t} d\mathrm{INactive}dt,$$

where *d*AHcedt is the rate of change (μmol/h) of tissue ChE enzyme, Ks is the zero-order enzyme synthesis rate (μmol/h), AHce is the amount (μmol) of available enzyme, Kd, Kr, and Ka are the 1st-order rates (hr^{-1}) for enzyme degradation, regeneration, and aging, respectively; Ki (μM/h) is the bimolecular rate of inhibition, INactive is the amount (μmol) of ChE that is inactivated due to phosphorylation of ChE. These equations were incorporated in all the model compartments (i.e., liver, brain, diaphragm, and blood) that contained B-EST activity.

One-compartment model TCP elimination. The pharmacokinetics of TCP in blood and urine were modeled utilizing a simple one-compartment analysis to describe blood and urinary elimination, where

$$\frac{dATCP}{dt} = \left(\sum \frac{dATCP(i)}{dt} \right) - (\mathrm{ATCP} * \mathrm{Ke}),$$

$$ATCP = \int_{0}^{t} d\mathrm{ATCP}dt,$$

$$\frac{dTCPexc}{dt} = \mathrm{ATCP} * \mathrm{Ke}$$

$$TCPexc = \int_{0}^{t} d\mathrm{TCPexc}dt,$$

$$\mathrm{cbTCP} = \frac{\mathrm{ATCP}}{\mathrm{Vd}},$$

*d*ATCPdt is the rate of change for TCP (μmol/h), in which *d*ATCP(i)dt is the rate of TCP formation from all sources (i.e., CYP450, A-EST, B-EST), ATCP is the amount of TCP (μmol), Ke is the 1st order (hr^{-1}) elimination rate constant, cbTCP is the blood concentration of TCP (μmol/h), and Vd is the volume of distribution (liter).

ACKNOWLEDGMENTS

We thank Dr. Richard A. Corley for his insightful discussion and advice in developing this PBPK/PD model and Drs. James C. Kisicki, Cindy Wilinson-Seip, and Michael L Comb from MDS Harris (Lincoln, NE) for conducting the human pharmacokinetic/pharmacodynamic studies. This work was supported through a contract with Dow AgroSciences, Indianapolis IN.

REFERENCES

Abbas, R., and Hayton, W. L. (1997). A physiologically based pharmacokinetic and pharmacodynamic model for paraoxon in rainbow trout. *Toxicol. Appl. Pharmacol.* **145,** 192–201.

Amitai, G., Moorad, D., Adani, R., and Doctor, B. P. (1998). Inhibition of acetylcholinesterase and butyrylcholinesterase by chlorpyrifos-oxon. *Biochem. Pharmacol.* **56,** 293–299.

Andersen, M. E. (1995). Development of physiologically based pharmacokinetic and physiologically based pharmacodynamic models for applications in toxicology and risk assessment. *Toxicol. Lett.* **79,** 35–44.

Andersen, M. E., Clewell, H. J., III, Gargas, M. L, Smith, F. A., and Reitz, R. H. (1987). Physiologically based pharmacokinetics and the risk assessment process for methylene chloride. *Toxicol. Appl. Pharmacol.* **87,** 185–205.

Aprea, C., Sciarra, G., Sartorelli, P., Desideri, E., Amati, R., and Sartorelli, E. (1994). Biological monitoring of exposure to organophosphorus insecticides by assay of urinary alkylphosphates: Influence of protective measures during manual operations with treated plants. *Int. Arch. Occup. Environ. Health* **66,** 333–338.

Bakke, J. E., Feil, V. J., and Price, C. E. (1976). Rat urinary metabolites from *O,O*-diethyl-*O*-(3,5,6-trichloro-2-pyridyl)phosphorothioate. *J. Environ. Sci. Health Bull.* **11,** 225–230.

Brown, R. P., Delp, M. D., Lindstedt, S. L., Rhomberg, L. R., and Beliles, R. P. (1997). Physiological parameter values for physiologically based pharmacokinetic models. *Toxicol. Ind. Health* **13,** 407–484.

Brzak, K. A., Harms, D. W., Bartels, M. J., and Nolan, R. J. (1998). Determination of chlorpyrifos, chlorpyrifos oxon, and 3,5,6-trichloro-2-pyridinol in rat and human blood. *J. Anal. Toxicol.* **22,** 203–210.

Butler, A. M., and Murray, M. (1997). Biotransformation of parathion in human liver: Participation of CYP3A4 and its inactivation during microsomal parathion oxidation. *J. Pharmacol. Exp. Ther.* **280,** 966–973.

Calabrese, E. J. (1991). Comparative metabolism: The principal causes of differential susceptibility to toxic and carcinogenic agents. In *Principles of Animal Extrapolation* (E. J. Calabrese, Ed.), pp. 203–276. Lewis Publishers, Chelsea, MI.

Carr, R. L., and Chambers, J. E. (1996). Kinetic analysis of the *in vitro* inhibition, aging and reactivation of brain acetylcholinesterase from rat and channel catfish by paraoxon and chlorpyrifos-oxon. *Toxicol. Appl. Pharmacol.* **139,** 365–373.

Chambers, J. E., and Chambers, J. W. (1989). Oxidative desulfuration of chlorpyrifos, chlorpyrifos-methyl, and leptophos by rat brain and liver. *J. Biochem. Toxicol.* **4,** 201–203.

Chan, L., Balabaskaran, S., Delilkan, A. E., and Ong, L. H. (1994). Blood cholinesterase levels in a group of Malaysian blood donors. *Malays. J. Pathol.* **16,** 161–164.

Chanda, S. M., Mortensen, S. R., Moser, V. C. and Padilla, S. (1997). Tissue-specific effects of chlorpyrifos on carboxylesterase and cholinesterase activity in adult rats: An *in vitro* and *in vivo* comparison. *Fundam. Appl. Toxicol.* **38,** 148–157.

Clement, J. G. (1984). Role of aliesterase in organophosphate poisoning. *Fundam. Appl. Toxicol.* **4,** S96–105.

Corley, R. A., Bormett, G. A., and Ghanayem, B. I. (1994). Physiologically

based pharmacokinetics of 2–butoxyethanol and its major metabolite, 2-butoxyacetic acid, in rats and humans. *Toxicol. Appl. Pharmacol*. **129,** 61–79.

Drevenkar, V., Vasilic, Z., Stengl, B., Frobe, Z., and Rumenjak, V. (1993). Chlorpyrifos metabolites in serum and urine of poisoned persons. *Chem. Biol. Interact.* **87,** 315–322.

Ecobichon, D. J., and Comeau, A. M. (1973). Pseudocholinesterases of mammalian plasma: Physiocochemical properties and organophosphate inhibition in eleven species. *Toxicol. Appl. Pharmacol*. **24,** 92–100.

Ellenhorn, M. J., and Barceloux, D. G. (1988*). Medical toxicology—Diagnosis and Treatment of Human poisoning*. Elsevier, New York.

Ellman, G. L., Courtney, K. D., Anders, V., Jr., and Geatherstone, R. M. (1961). A new and rapid colorimetric determination of acetylcholinesterase activity. *Biochem. Pharmacol*. **7,** 88–95.

Fabrizi, L., Gemma, S., Testai, E., and Vittozzi, L. (1999). Identification of the cytochrome P450 isoenzymes involved in the metabolism of diazinon in the rat liver. *J. Biochem. Mol. Toxicol.* **13**, 53–61.

Gaines, T. B. (1969). Acute toxicity of pesticides. *Toxicol. Appl. Pharmacol*. **14,** 515–534.

Gearhart, J. M., Jepson, G. W., Clewell, H. J., III, Andersen, M. E., and Conolly, R. B. (1990). Physiologically based pharmacokinetic and pharmacodynamic model for the inhibition of acetylcholinesterase by diisopropylfluorophosphate. *Toxicol. Appl. Pharmacol*. **106,** 295–310.

Gibson, J. E., Chen, W. L., and Peterson, R. K. D. (1999). How to determine if an additional 10× safety factor is needed for chemicals: A case study with chlorpyrifos. *Toxicol. Sci*. **48,** 117–122.

Griffin, P., Mason, H., Heywood, K., and Cocker, J. (1999). Oral and dermal absorption of chlorpyrifos: A human volunteer study. *Occup. Environ. Med*. **56,** 10–13.

Guengerich, F. P. (1977). Separation and purification of multiple forms of microsomal cytochrome P-450. Activities of different forms of cytochrome P-450 towards several compounds of environmental interest. *J. Biol. Chem.* **252,** 3970–3979.

Hall, S. D., Thummel, K. E., Watkins, P. B., Lown, K. S., Benet, L. Z., Paine, M. F., Mayo, R. R., Turgeon, D. K., Bailey, D. G., Fontana, R. J., and Wrighton, S. A. (1999). Molecular and physical mechanisms of first-pass extraction. *Drug Metab. Dispos.* **27,** 161–166.

Hill, R. H., Head, S. L., Baker, S., Gregg, M., Shealy, D. B., Bailey, S. L., Williams, C. C., Sampson, E. J., and Needham, L. L. (1995). Pesticide residues in urine of adults living in the United States: Reference range concentrations. *Environ. Res.* **71,** 99–108.

Jochemsen, R., Bazot, D., Brillanceau, M. H., and Lupart, M. (1993). Assessment of drug exposure in rat dietary studies. *Xenobiotica* **23,** 1145–1154.

Kararli, T. T. (1995). Comparison of the gastrointestinal anatomy, physiology, and biochemistry of humans and commonly used laboratory animals. *Biopharm. Drug Dispos*. **16,** 351–380.

Lanning, C. L., Fine, R. L., Sachs, C. W., Rao, U. S., Corcoran, J. J., and Abou-Donia, M. B. (1996). Chlorpyrifos oxon interacts with the mammalian multidrug-resistance protein, P-glycoprotein. *J. Toxicol. Environ. Health* **47,** 395–407.

Loewenherz, C., Fenske, R. A., Simcox, N. J., Bellamy, G., and Kalman, D. (1997). Biological monitoring of organophosphorus pesticide exposure among children of agricultural workers in central Washington state. *Environ. Health Perspect.* **105,** 1344–1353.

Lotti, M., Moretto, A., Zoppellari, R., Dainese, R., Rizzuto, N., and Barusco, G. (1986). Inhibition of lymphocytic neuropathy target esterase predicts the development of organophosphate-induced delayed polyneuropathy. *Arch. Toxicol.* **59,** 176–179.

Ma, T., and Chambers, J. E. (1994). Kinetic parameters of desulfuration and dearylation of parathion and chlorpyrifos by rat liver microsomes. *Food Chem. Toxicol.* **32,** 763–767.

Ma, T., and Chambers, J. E. (1995). A kinetic analysis of hepatic microsomal activation of parathion and chlorpyrifos in control and phenobarbital-treated rats. *J. Biochem. Toxicol.* **10**, 63–68.

Maxwell, D. M., Lenz, D. E., Groff, W. A., Kaminskis, A., and Froehlich, H. L. (1987). The effect of blood flow and detoxification on *in vivo* cholinesterase inhibition by soman in rats. *Toxicol. Appl. Pharmacol*. **88,** 66–76.

Maxwell, D. M., Vlahacos, C. P., and Lenz, D. E. (1988). A pharmacodynamic model for soman in the rats. *Toxicol. Lett*. **43,** 175–188.

McCollister, S. B., Kociba, R. J., Humiston, C. G., and McCollister, D. D. (1974). Studies on the acute and long-term oral toxicity of chlorpyrifos (*o,o*-diethyl-o-(3,5,6-trichloro-2-pyridyl) phosphorothioate). *Food Cosmet. Toxicol*. **12,** 45–61.

McDougal, J. N., Jepson, G. W., Clewell, H. J., III, MacNaughton, M. G., and Andersen, M. E. (1986). A physiological pharmacokinetic model for dermal absorption of vapors in the rat. *Toxicol. Appl. Pharmacol.* **85,** 286–294.

Mortensen, S. R., Brimijoin, S., Hooper, M. J., and Padilla, S. (1998). Comparison of the *in vitro* sensitivity of rat acetylcholinesterase to chlorpyrifos-oxon: What do tissue IC_{50} values represent? *Toxicol. Appl. Pharmacol*. **148,** 46–49.

Mortensen, S. R., Chanda, S. M., Hooper, M. J., and Padilla, S. (1996). Maturational differences in chlorpyrifos-oxonase activity may contribute to age-related sensitivity to chlorpyrifos. *J. Biochem. Toxicol*. **11,** 279–287.

Murphy, S. D. (1986). Toxic effects of pesticides. In *Casarett and Doull's Toxicology, The Basic Science of Poison*, 3rd ed. (C. D. Klaassen, M. O. Amdur, and J. Doull, Eds.), pp. 519–581. MacMillam, New York.

Neal, R. A. (1980). Microsomal metabolism of thiono-sulfur compounds, mechanisms, and toxicological significance. In *Reviews in Biochemical Toxicology* (E. Hodgson, J. R. Bend, and R. M. Philpot, Eds.) Vol. 2, pp. 131–172. Elsevier-North Holland, New York.

Nolan, R. J., Rick, D. L., Freshour, N. L., and Saunders, J. H. (1984). Chlorpyrifos: Pharmacokinetics in human volunteers. *Toxicol. Appl. Pharmacol.* **73,** 8–15.

Nostrandt, A. C., Padilla, S., and Moser, V. C. (1997). The relationship of oral chlorpyrifos: Effects on behavior, cholinesterase inhibition, and muscarinic-receptor density in rat. *Pharmacol. Biochem. Behav*. **58**, 15–23.

Obach, R. S., Zhang, Q.-Y., Dunbar, D., and Kaminsky, L. S. (2001). Metabolic characterization of the major human small intestinal cytochrome P450s. *Drug Metab. Dispos*. **29**, 347–352.

ORNL (2000). Appendix G: Inhibition of cholinesterases and an evaluation of the methods used to measure cholinesterase activity. Oak Ridge National Laboratory. *J. Toxicol. Environ. Health A* **59,** 519–526.

Paine, M. F., Schmiedlin-Ren, P., and Watkins, P. B. (1999). Cytochrome P-450 1A1 expression in human small bowel: Interindividual variation and inhibition by ketoconazole. *Drug Metab. Dispos*. **27**, 360–364.

Poet, T. S. (2000). Assessing dermal absorption. *Toxicol. Sci*. **58,** 1–2.

Poet, T. S., Corley, R. A., Thrall, K. D., Edwards, J. A., Tanojo, H., Weitz, K. K., Hui, X., Maibach, H. I., and Wester, R. C. (2000). Assessment of the percutaneous absorption of trichloroethylene in rats and humans using MS/MS real-time breath analysis and physiologically based pharmacokinetic modeling. *Toxicol. Sci*. **56,** 61–72.

Pond, A. L., Chambers, H. W., and Chambers, J. E. (1995). Organophosphate detoxification potential of various rat tissues via A-esterase and aliesterase activity. *Toxicol. Lett.* **78,** 245–252.

Poulin, P., and Krishnan, K. (1995). An algorithm for predicting tissue: blood partition coefficients of organic chemicals from n-octonol: Water partition coefficient data. *J. Toxicol. Environ. Health* **46,** 117–129.

Quackenboss, J. J., Pellizari, E., Freeman, N., Head, S., Whitmore, R., Zelan, H., and Stroebel, C. (1998). *Use of Screening Questionnaires to Identify Exposed and Sensitive Population Groups in the Region V NHEXAS Children's Pesticide Study.* Presented at the Tenth Conference of the Interna-

tional Society of Environmental Epidemiology and Eighth Conference of the International Society of Exposure Analysis, Boston.

Ramsey, J. C., and Andersen, M. E. (1984). A physiologically based description of the inhalation pharmacokinetics of styrene in rats and humans. *Toxicol. Appl. Pharmacol*. **73,** 159–175.

Renwick, A. G. (1994). Toxicokinetics-pharmacokinetics in toxicology. In *Principles and Methods of Toxicology*, 3rd ed. (A. W. Hayes, Ed.), pp. 101–147. Raven Press, New York.

Richter, E. D., Kowalski, M., Leventhal, A., Grauer, F., Marzouk, J., Brenner, S., Shkolnik, I., Lerman, S., Zahavi, H., Bashari, A., Peretz, A., Kaplanski, H., Gruener, N., and Ben Ishai, P. (1992). Illness and excretion of organophosphate metabolites four months after household pest extermination. *Arch. Environ. Health* **47,** 135–138.

Sams, C., Mason, H. J., and Rawbone, R. (2000). Evidence for the activation of organophosphate pesticides by cytochromes P450 3A4 and 2D6 in human liver microsomes. *Toxicol. Lett.* **116,** 217–221.

Schalm, O. W., Ed. (1961). *Veterinary hematology*. Lea and Febiger, Philadelphia, PA.

Schmiedlin-Ren, P., Benedict, P. E., Dobbins, W. O., III, Ghosh, M., Kolars, J. C., and Watkins, P. B. (1993). Cultured adult rat jejunal explants as a model for studying regulation of CYP3A. *Biochem. Pharmacol*. **46**, 905–918.

Shurdut, B. A., Barraj, L., and Francis, M. (1998). Aggregate exposures under the Food Quality Protection Act: An approach using chlorpyrifos. *Regul. Toxicol. Pharmacol*. **28,** 165–177.

Staats, D. A., Fisher, J. W., and Conolly, R. B. (1991). Gastrointestinal absorption of xenobiotics in physiologically based pharmacokinetic models. A two-compartment description. *Drug Metab. Disp*. **19,** 144–148.

Sultatos, L. G. (1990). A physiologically based pharmacokinetic model of parathion based on chemical-specific parameters determined *in vitro*. *J. Amer. Coll. Toxicol.* **9,** 611–619.

Sultatos, L. G. (1994). Mammalian toxicology of organophosphorus pesticides. *J. Toxicol. Environ. Health* **43,** 271–289.

Sultatos, L. G., and Murphy, S. D. (1983). Kinetic analyses of the microsomal biotransformation of the phosphorothioate insecticides chlorpyrifos and parathion. *Fundam. Appl. Toxicol.* **3,** 16–21.

Sultatos, L. G., Shao, M., and Murphy, S. D. (1984). The role of hepatic biotransformation in mediating the acute toxicity of the phosphorothionate insecticide chlorpyrifos. *Toxicol. Appl. Pharmacol.* **73,** 60–68.

U. S. EPA (1998). Health effects of pesticides. In *The EPA Children's Environmental Health Yearbook*, U. S. Environmental Protection Agency, Office of Children's Health Protection.

Vale, J. A. (1998). Toxicokinetic and toxicodynamic aspects of organophosphate (OP) insecticide poisoning. *Toxicol. Lett*. **102–103,** 649–652.

Vasilic, Z., Drevenkar, V., Rumenjak, V., Stengl, B., and Frobe, Z. (1992). Urinary excretion of diethylphosphorus metabolites in persons poisoned by quinalphos or chlorpyrifos. *Arch. Environ. Contam. Toxicol*. **22,** 351–357.

Venkataraman, B. V., and Rani, M. A. (1994). Species variation in the specificity of cholinesterases in human and rat blood samples. *Indian J. Physiol. Pharmacol.* **38,** 211–213.

Watkins, P. B. (1992). Drug metabolism by cytochromes P450 in the liver and small bowel. *Gastroenterol. Clin. North Am*. **21,** 511–526.

Wester, R. C., Maibach, H. I., Bucks, D. A. W., and Guy, R. H. (1983). Malathion percutaneous absorption after repeated administration to man. *Toxicol. Appl. Pharmacol*. **68,** 116–119.

Wester, R. C., Maibach, H. I., Melendres, J., Sedik, L., Knaak, J., and Wang, R (1992). *In vivo* and *in vitro* percutaneous absorption and skin evaporation of isofenphos in man. *Fundam. Appl. Pharmacol.* **19,** 521–526.

Wester, R. C., Sedik, L., Melendres, J., Logan, F., Maibach, H. I., and Russell, I. (1993). Percutaneous absorption of diazinon in humans. *Food Chem. Toxicol.* **31,** 569–572.

Withey, J. R., Collins, B. T., and Collins, P. G. (1983). Effect of vehicle on the pharmacokinetics and uptake of four halogenated hydrocarbons from the gastrointestinal tract of the rat. *J. Appl. Toxicol*. **3,** 249–253.

Yano, B. L., Young, J. T., and Mattsson, J. L. (2000) Lack of carcinogenicity of chlorpyrifos insecticide in a high-dose, 2-year dietary toxicity study in Fischer 344 rats. *Toxicol. Sci*. **53,** 135–144.

Zhang, Q.-Y., Dunbar, D., Ostrowska, A., Zeisloft, S., Yang, J., and Kaminsky, L. S. (1999). Characterization of human small intestinal cytochromes P-450. *Drug Metab. Dispos*. **27**, 804–809.

Zheng, Q., Olivier, K., Won, Y. K., and Pope, C. N. (2000). Comparative cholinergic neurotoxicity of chlorpyrifos exposures in pre-weanling and adult rats. *Toxicol. Sci*. **55,** 124–132.